

RECEIVED: January 6, 2023

REVISED: March 22, 2023

ACCEPTED: March 23, 2023

PUBLISHED: April 6, 2023

Electroweak-flavour and quark-lepton unification: a family non-universal path

Joe Davighi, Gino Isidori and Marko Pesut

*Physik-Institut, Universität Zürich,
Winterthurerstrasse 190, CH 8057 Zürich, Switzerland*

E-mail: joe.davighi@physik.uzh.ch, isidori@physik.uzh.ch,
marko.pesut@physik.uzh.ch

ABSTRACT: We present a family-non-universal extension of the Standard Model where the first two families feature both quark-lepton and electroweak-flavour unification, via the $SU(4) \times Sp(4)_L \times Sp(4)_R$ gauge group, whereas quark-lepton unification for the third family is realised à la Pati-Salam. Via staggered symmetry breaking steps, this construction offers a natural explanation for the observed hierarchical pattern of fermion masses and mixings, while providing a natural suppression for flavour-changing processes involving the first two generations. The last-but-one step in the symmetry-breaking chain is a non-universal 4321 model, characterised by a vector leptoquark naturally coupled mainly to the third generation. The stability of the Higgs sector points to a $4321 \rightarrow SM$ symmetry-breaking scale around the TeV, with interesting phenomenological consequences in B physics and collider processes that differ from those of other known 4321 completions.

KEYWORDS: Theories of Flavour, Grand Unification, Vector-Like Fermions, Hierarchy Problem

ARXIV EPRINT: [2212.06163](https://arxiv.org/abs/2212.06163)

Contents

1	Introduction	1
2	A new flavoured gauge model	4
2.1	Mathematical notation and conventions	4
2.2	Embedding the Standard Model fields	6
2.3	Fundamental Yukawa interactions	7
3	Dynamical generation of the Yukawa sector	8
3.1	Electroweak light-flavour unification	8
3.1.1	Sequential symmetry breaking (part I)	8
3.1.2	EFT matching for light Yukawas	11
3.2	Mixing with the third family	13
3.2.1	Sequential symmetry breaking (part II)	13
3.2.2	EFT matching for third family Yukawas and mixings	16
3.3	Fermion mass and mixing angle observables	19
4	Anchoring the low scale	19
4.1	The light-Higgs sector	19
4.1.1	Mixing and spectrum in the light-Higgs sector	20
4.1.2	Constraints on the scales from the electroweak vacuum	22
4.2	Leptoquark phenomenology	22
4.2.1	$R_{D^{(*)}}$ and $pp \rightarrow \tau^+ \tau^- + X$	24
4.2.2	$R_{K^{(*)}}$	25
5	Conclusion and outlook	27
A	Formulae for fermion masses and mixing angles	29
B	Basis of $\text{Sp}(4)$ generators	31

1 Introduction

The Standard Model (SM) of particle physics is currently the most accurate theoretical framework to describe microscopic phenomena. The SM successfully passed several precision tests, and no new degrees of freedom have emerged yet by the direct exploration of the TeV energy domain at the LHC. Nevertheless, the SM is plagued by a significant number of open issues. The two we deal with in this paper, namely the *flavour puzzle* and the possible *unification* of quarks and leptons, are related to the matter content of the SM. The flavour puzzle refers to the highly non-generic pattern of masses and mixings of the three families

of quarks and leptons, which has no justification within the SM. Equally puzzling is the peculiar assignment of the $U(1)_Y$ charges for the SM fermions that, despite being justified *a posteriori* by the requirement of anomaly cancellation, naturally points toward some form of unification of quark and lepton quantum numbers at high energies.

Attempts to provide dynamical justifications of the flavour puzzle, and attempts to unify quarks and leptons into representations of new (non-Abelian) gauge groups, both have a long history. However, to a large extent, these two efforts proceeded in parallel until recently. Unification was pursued in a flavour-blind manner, extending the SM gauge group into a grand-unified group acting in the same way for the three fermion generations [1]. The flavour problem was addressed via appropriate horizontal symmetries (global or gauged, continuous or discrete), commuting with the aforementioned unified gauge symmetry, as proposed for instance in [2]. The factorisation of flavour and gauge symmetries was phenomenologically motivated by the universality of the SM gauge group and, to some extent, by simplicity. But it is certainly not the only option. The path we explore in this paper is a different one: it is based on the assumption that the gauge group in the ultraviolet (UV) is fundamentally family non-universal.

In the case of family non-universal gauge groups, the flavour problem is addressed via a cascade of symmetry breaking steps occurring at different energy scales, from the initial non-universal group to more universal ones, eventually ending with the SM, as in [3–8]. Qualitatively, the light families are generated at some high scale, where the non-universality of the light families becomes manifest (i.e. at the scale where the light fermions have new, non-universal, dynamical interactions). This implies a suppression with respect to the third generation Yukawa couplings, which are generated at a lower scale. This type of construction potentially addresses also another key open issue of the SM: a (stable) separation of the scale stabilising the Higgs sector and the scale of new dynamics affecting the light families. With such separation, the new dynamics stabilising the Higgs sector, which necessarily couples strongly also to the third family, can still be quite close to the TeV scale while avoiding (at least in part) the tight constraints derived from processes involving the light families.

In addition to these general (top-down) arguments, interest in family non-universal gauge groups has arisen recently from a pure bottom-up perspective because of the B -physics anomalies, i.e. the deviations from the SM predictions observed in semileptonic B -meson decays (see [9] and references therein). An interesting hypothesis describing well all present data is the extension of the SM field content by a massive vector leptoquark field (U_1), in the TeV mass range, coupled mainly to the third generation [10]. The U_1 field has the right couplings and quantum numbers to be the broken generator of a (non-universal) $SU(4)_3$ group acting on the third family. This, in turn, has led to the so-called 4321 models: a construction based on the (TeV-scale) gauge symmetry $SU(4)_3 \times SU(3)_l \times SU(2)_L \times U(1)_X$ [5, 11, 12], where $SU(3)_l$ acts only on the light families and color is the family diagonal subgroup of $SU(4)_3 \times SU(3)_l$. Besides offering a successful description of the B -physics anomalies, this set-up features i) quark and lepton unification à la Pati-Salam [13] for the third generation, and ii) an accidental $U(2)^5$ global flavour symmetry acting on the light families. The latter is known to be an excellent first-order approximation to the SM Yukawa couplings

and, if broken in a minimal way, a key ingredient to ensuring sufficient protection against flavour-violating effects involving the light families [14, 15].

It is natural to try to merge the indication of a 4321 gauge group at the TeV scale with the more general top-down considerations about non-universal gauge groups presented above. From this perspective, the 4321 group should be viewed as the last-but-one step of the symmetry breaking chain from the UV theory down to the SM. Attempts of this type have been presented in [5, 8, 16, 17]. In this paper we present a new proposal along this line, which is significantly different from all previous attempts.

The novel aspect of our construction is the concept of *electroweak-flavour unification*, which invokes an $\text{Sp}(2N_f)_L \times \text{Sp}(2N_f)_R$ gauge symmetry (in the general case of N_f families), recently proposed in [18]. Rather than imposing this structure to unify all three fermion families, as suggested in [18], we here propose a different path for light *vs.* heavy families: both sectors feature quark-lepton unification via independent $\text{SU}(4)$ groups, while only the light sector features electroweak-flavour unification via $\text{Sp}(4)_L \times \text{Sp}(4)_R$. With this proposal the separation between the third family and the other two is “hard-coded” in the UV, where the gauge symmetry is the direct product of groups acting separately on the different fermion sectors. This is a good premise to justify in a natural way the large mixing occurring in the light family sector, controlled by the Cabibbo angle ($|V_{us}| \sim 0.2$), *vs.* the small heavy-light mixing controlled by $|V_{ts}| \sim 0.04$. As we shall see, assuming a sufficiently high-scale for the $\text{Sp}(2N_f)_L \times \text{Sp}(2N_f)_R$ symmetry breaking, this set-up also provides a natural justification for the minimal breaking of the $\text{U}(2)^5$ flavour symmetry [14], which ensures an efficient suppression of non-SM effects in flavour-changing processes involving the light families.¹

The mixing between the two sectors happens via scalar fields charged under both gauge groups, and appropriate vector-like fermions. While the observed flavour hierarchies (masses and mixings) fix only the ratios between the different scales of this construction, an absolute indication of the new energy scales comes from the stability of the field combination responsible for electroweak symmetry breaking, i.e. the effective SM Higgs sector. The latter requires the lowest non-standard symmetry breaking step (4321 \rightarrow SM) to occur around the TeV scale. This is a further indication for new dynamics coupled mainly to the third generation in this energy domain, independent from that obtained from the *B*-physics anomaly. As we shall show, in this framework the data-theory comparison in *B*-physics improves, but the low-energy signatures of the model are different from those derived in the other known 4321 completions. This fact, together with the specific TeV-scale phenomenology of the model, could help in the future to identify this motivated scenario.

The paper is organised as follows. In section 2 we introduce the UV gauge group as well as the matter content of the model. We discuss the symmetry breaking pattern and briefly review some basic facts about $\text{Sp}(4)$ Lie groups. In section 3 we present a detailed derivation of the Yukawa couplings for all the SM fermions. Section 4 is devoted to the last step of the symmetry breaking chain, which allow us to anchor the various scales of

¹Arguably, a $\text{U}(2)^5$ flavour symmetry appears even more motivated after the recent $R_{K^{(*)}}$ measurement by the LHCb collaboration [19], which provides a further strong constraint on non-universality between the two light lepton generations.

the model from the stability of the Higgs sector. In this section we also derive predictions for both B -physics and collider phenomenology. Finally, we conclude and discuss some interesting future directions in section 5.

2 A new flavoured gauge model

The model we propose is based on a high-energy gauge group that treats the third family differently from the light two families, which are tightly unified. The gauge group has the form

$$G = G_{12} \times G_3, \tag{2.1}$$

with the light families charged only under G_{12} and the third family charged only under G_3 . As described in the Introduction, such a factorization of the gauge sector is strongly-motivated by the observed Yukawa sector alone, together with considerations of naturalness and data from high p_T .

Guided by our desire for a third-family aligned U_1 leptoquark, we then take

$$G_3 = \text{SU}(4)_3 \times \text{SU}(2)_{L,3} \times \text{SU}(2)_{R,3} \tag{2.2}$$

to be a Pati-Salam symmetry. For the light families we also unify quarks with leptons à la Pati-Salam, while further unifying the electroweak and flavour quantum numbers in the manner recently explored for all three families in ref. [18]. We thus consider²

$$G_{12} = \text{SU}(4)_{1+2} \times \text{Sp}(4)_L \times \text{Sp}(4)_R, \tag{2.3}$$

where $\text{Sp}(4)$ denotes the symplectic group (see section 2.1). More minimal choices for G_{12} and G_3 could have been made, for example $G_3 = \text{SM}_3$ and $G_{12} = \text{SU}(3)_{1+2} \times \text{Sp}(4)_L \times \text{Sp}(4)_R \times \text{U}(1)_{B-L,1+2}$, if we do not wish to unify quarks and leptons. The choices (2.2) and (2.3) for G_3 and G_{12} are motivated by matter unification in the UV, in particular absorbing $\text{U}(1)$ factors in the gauge symmetry, plus the phenomenological interest in vector leptoquarks near the TeV scale.

2.1 Mathematical notation and conventions

In our convention, $\text{Sp}(4) \subset \text{SU}(4)$ is the 10-dimensional group of 4×4 special unitary matrices $\{U\}$ that moreover satisfy $U^T \Omega U = \Omega$, where the matrix

$$\Omega = \begin{pmatrix} 0 & \mathbb{I}_2 \\ -\mathbb{I}_2 & 0 \end{pmatrix}, \tag{2.4}$$

with \mathbb{I}_2 being the 2-by-2 identity matrix. The Lie algebra $\mathfrak{sp}(4)$ and its representations are probably familiar to most readers, thanks to the Lie algebra isomorphism $\mathfrak{sp}(4) \cong \mathfrak{so}(5)$. The corresponding Lie group isomorphism is $\text{Sp}(4) \cong \text{Spin}(5)$, where $\text{Spin}(5)$ is the double cover of $\text{SO}(5)$.

²We remark that $\mathfrak{g} = \text{Lie}(G)$ is listed as algebra number 157 in ref. [20] (supplementary material), which comprehensively studied semi-simple gauge algebras with possible gauge-flavour unification.

To set out a little more necessary notation, we let $\{a_1, a_2, a_3, a_4\}$ denote a basis for the \mathbb{C}^4 vector space acted on by the fundamental representation $\mathbf{4}$ of $SU(4)_{1+2}$, with $\{a_i^*\}$ a basis for the conjugate $\bar{\mathbf{4}}$ representation; correspondingly, let $\{A_i\}$ and $\{A_i^*\}$ denote bases for the fundamental and anti-fundamental representations of $SU(4)_3$. We let $\{b_1, \dots, b_4\}$ and $\{c_1, \dots, c_4\}$ denote bases for the vector spaces (both \mathbb{C}^4) acted on by the fundamental of $Sp(4)_L$ and $Sp(4)_R$ respectively, and $\{B_1, B_2\}$, $\{C_1, C_2\}$ denote the bases for the \mathbb{C}^2 vector spaces acted on by the fundamental representations of $SU(2)_{L,3}$ and $SU(2)_{R,3}$.

For $Sp(2n)$ groups, like for $SU(2) \cong Sp(2)$, the fundamental and its conjugate representation are isomorphic. It is therefore convenient to introduce a notion of complex conjugation $(*)$ that, in addition to sending all \mathbb{C} -valued components to their ordinary complex conjugates, acts on our basis vectors as $* : b_i \mapsto \Omega_{ji} b_j$ and $* : c_i \mapsto \Omega_{ji} c_j$. With this definition, the conjugate φ^* of some field φ transforming in the $\mathbf{4}$ of $Sp(4)$ also transforms in the $\mathbf{4}$.³ For the $n = 1$ case, the factor of Ω appearing in the automorphism $*$ is the familiar factor of $i\sigma_2$ that conventionally appears in complex conjugation of $SU(2)$ doublets.

The Ω matrices provide invariant tensors for symplectic groups, which we can use to construct singlets. In particular, given two fields $x = x_i b_i$ and $y = y_i b_i$ in the fundamental representation of $Sp(4)$, the contraction

$$x_i \Omega^{ij} y_j \tag{2.5}$$

is an $Sp(4)$ singlet. We will frequently encounter such contractions of $Sp(4)$ fundamentals in the following, where we always suppress writing the indices and the requisite insertions of the Ω matrix (which are implied). Other than the fundamental, all the representations of $Sp(4)$ that feature in this paper appear in the tensor product of two fundamentals, which is

$$\mathbf{4} \otimes \mathbf{4} = \mathbf{1} \oplus \mathbf{5} \oplus \mathbf{10}. \tag{2.6}$$

Here, the $\mathbf{10}$ is the *symmetric* contraction of two fundamentals, which for $Sp(2N)$ Lie groups is isomorphic to the *adjoint* representation, and the $\mathbf{5}$ is the part of the *antisymmetric* contraction that remains after subtracting off the singlet (2.5).

We also introduce a convenient notation to indicate the ‘flow’ of $Sp(4)$ indices in Feynman diagrams, following [18], whereby solid red lines (—) marked with one or two arrows denote specific contractions of $Sp(4)_L$ fundamental representations x and y . The number of arrows matches the family of the SM fermions involved in the contraction:

$$\begin{aligned} [x \xrightarrow{\hspace{1.5cm}} y] &\sim x_1 y_3 & [x \xleftarrow{\hspace{1.5cm}} y] &\sim x_3 y_1 \\ [x \xrightarrow{\hspace{1.5cm}}\!\!\!\rightarrow y] &\sim x_2 y_4 & [x \xleftarrow{\hspace{1.5cm}}\!\!\!\leftarrow y] &\sim x_4 y_2 \end{aligned}$$

Similarly, dashed blue lines (---) will be used to represent $Sp(4)_R$ contractions.

³To see this explicitly, let $\varphi = \varphi_i b_i$ denote a field in the fundamental $\mathbf{4}$ of $Sp(4)$. Under the $Sp(4)$ action, $\varphi_i \mapsto U_{ij} \varphi_j$, where U_{ij} are the components of a 4-by-4 $Sp(4)$ matrix. The conjugate field φ^* has components $(\varphi^*)_i = \Omega_{ij} \varphi_j^*$ with respect to the same basis $\{b_i\}$. Under $Sp(4)$, $(\varphi^*)_i \mapsto \Omega_{ij} U_{jk}^* \varphi_k^* = U_{ij} \Omega_{jk} \varphi_k^* = U_{ij} (\varphi^*)_j$, where we have used $U^T \Omega U = \Omega$. Thus (φ^*) and φ transform in the same $\mathbf{4}$ representation.

	Field	SU(4) ₁₊₂	Sp(4) _L	Sp(4) _R	SU(4) ₃	SU(2) _{L,3}	SU(2) _{R,3}
SM Fermions (chiral)	Ψ_L^l	4	4	1	1	1	1
	Ψ_R^l	4	1	4	1	1	1
	Ψ_L^3	1	1	1	4	2	1
	Ψ_R^3	1	1	1	4	1	2
Vector-like fermion	$\Xi_{L/R}$	4	1	4	1	1	1
EWSB Higgses	\mathcal{H}_1	1	4	4	1	1	1
	\mathcal{H}_{15}	15	4	4	1	1	1
	H_1	1	1	1	1	2	2
	H_{15}	1	1	1	15	2	2
Symmetry breaking scalars	S_L	1	5	1	1	1	1
	S_R	$\bar{\mathbf{4}}$	1	4	1	1	1
	Φ_L	1	5	1	1	1	1
	Φ_R	1	1	5	1	1	1
	Σ_L	1	4	1	1	2	1
	Σ_R	1	1	4	1	1	2
	ω	4	1	4	$\bar{\mathbf{4}}$	1	2

Table 1. Field content of the model. In addition to the SM fermions, there are various scalar fields in which the electroweak symmetry breaking Higgs fields are embedded, as well as other symmetry breaking scalars that break the gauge symmetry down to the SM, plus a vector-like fermion.

2.2 Embedding the Standard Model fields

The light fermion fields of the SM are all packaged into two 16-component reps, $\Psi_L^l \sim (\mathbf{4}, \mathbf{4}, \mathbf{1}) \otimes (\mathbf{1}, \mathbf{1}, \mathbf{1})$ which is left-handed and $\Psi_R^l \sim (\mathbf{4}, \mathbf{1}, \mathbf{4}) \otimes (\mathbf{1}, \mathbf{1}, \mathbf{1})$ which is right-handed, where the label ‘ l ’ stands for ‘light’. We can represent Ψ_L^l and Ψ_R^l as 4×4 matrices whose rows transform in the fundamental representation of $\text{Sp}(4)_L$ and $\text{Sp}(4)_R$ respectively, and whose columns transform in the fundamental of $\text{SU}(4)_{1+2}$, viz.

$$\Psi_L^l = \begin{pmatrix} u_{1,L}^r & u_{2,L}^r & d_{1,L}^r & d_{2,L}^r \\ u_{1,L}^g & u_{2,L}^g & d_{1,L}^g & d_{2,L}^g \\ u_{1,L}^b & u_{2,L}^b & d_{1,L}^b & d_{2,L}^b \\ \nu_{1,L} & \nu_{2,L} & e_{1,L} & e_{2,L} \end{pmatrix}, \quad \Psi_R^l = \begin{pmatrix} u_{1,R}^r & u_{2,R}^r & d_{1,R}^r & d_{2,R}^r \\ u_{1,R}^g & u_{2,R}^g & d_{1,R}^g & d_{2,R}^g \\ u_{1,R}^b & u_{2,R}^b & d_{1,R}^b & d_{2,R}^b \\ \nu_{1,R} & \nu_{2,R} & e_{1,R} & e_{2,R} \end{pmatrix}, \quad (2.7)$$

where $u_{i,L}^a$ denotes a left-handed up quark with colour a and family index i , etc. With this chiral fermion content, our gauge model is free of both perturbative and non-perturbative gauge anomalies.⁴

There are Higgs fields that couple to both light families, in the representations $\mathcal{H}_1 \sim (\mathbf{1}, \mathbf{4}, \mathbf{4}) \otimes (\mathbf{1}, \mathbf{1}, \mathbf{1})$ and $\mathcal{H}_{15} \sim (\mathbf{15}, \mathbf{4}, \mathbf{4}) \otimes (\mathbf{1}, \mathbf{1}, \mathbf{1})$, as well as separate Higgs fields $H_1 \sim$

⁴The $\text{SU}(4)$ factors have possible perturbative gauge anomalies, but these cancel because there are equal numbers of left- and right-handed Weyl fermions in the (anomalous) fundamental representations of each $\text{SU}(4)$. The $\text{Sp}(4)$ and $\text{SU}(2)$ factors can suffer at most mod 2 anomalies in 4d [21], since these groups only have real and pseudo-real representations. Given that we have even numbers of Weyl fermions charged in the fundamental representation of each $\text{Sp}(4)$ and $\text{SU}(2)$ factor, all these mod 2 anomalies cancel. Finally, one can rigorously check that there are no further possible non-perturbative anomalies by computing the spin-bordism group $\Omega_5^{\text{Spin}}(B(G_{12} \times G_3)) \cong (\mathbb{Z}_2)^4$, using e.g. the methods of refs. [22, 23].

$(\mathbf{1}, \mathbf{1}, \mathbf{1}) \otimes (\mathbf{1}, \mathbf{2}, \mathbf{2})$ and $H_{15} \sim (\mathbf{1}, \mathbf{1}, \mathbf{1}) \otimes (\mathbf{15}, \mathbf{2}, \mathbf{2})$ that couple to the third family. It will be the latter Higgs fields, H_1 and H_{15} , that acquire non-zero vacuum expectation values (vevs) which break electroweak symmetry and, via mixing with \mathcal{H} (see section 4), mediate the light Yukawa couplings.

The representations of all SM fields are recorded in table 1, along with all the extra fields (many scalars and one vector-like fermion) that will feature in the model.

2.3 Fundamental Yukawa interactions

The renormalisable Yukawa couplings between the SM fermions and these various Higgs fields are

$$\begin{aligned}
 -\mathcal{L} \supset & \sum_{a \in \{1,15\}} \left[y_a^l \text{Tr} (\bar{\Psi}_L^l \mathcal{H}_a \Psi_R^l) + \bar{y}_a^l \text{Tr} (\bar{\Psi}_L^l \mathcal{H}_a^* \Psi_R^l) \right] \\
 & + \sum_{a \in \{1,15\}} \left[y_a^3 \text{Tr} (\bar{\Psi}_L^3 H_a \Psi_R^3) + \bar{y}_a^3 \text{Tr} (\bar{\Psi}_L^3 H_a^* \Psi_R^3) \right] + \text{h.c.} \quad (2.8)
 \end{aligned}$$

The terms in the first line couple the light fermions $\Psi_{L,R}^l$ to the \mathcal{H}_a Higgs fields. The terms in the second line couple the third family fermions $\Psi_{L,R}^3$ to the H_a Higgs fields.

The model will also feature a vector-like fermion (VLF) in the representation $\Xi \sim (\mathbf{4}, \mathbf{1}, \mathbf{4}) \otimes (\mathbf{1}, \mathbf{1}, \mathbf{1})$, charged only under the light-flavour group — specifically, in the same representation as Ψ_R^l . This VLF is needed to introduce mixing between the third family SM fermions and the light generations, as discussed in section 3.2.2. There are additional renormalisable Yukawa interactions involving Ξ , some with the \mathcal{H}_a Higgs fields, and others with the scalar field $\omega \sim (\mathbf{4}, \mathbf{1}, \mathbf{4}) \otimes (\bar{\mathbf{4}}, \mathbf{1}, \mathbf{2})$ (see table 1) that will play a role in breaking the UV gauge symmetry down to the SM. These extra Yukawa interactions are

$$\begin{aligned}
 -\mathcal{L} \supset & \lambda \text{Tr} (\bar{\Xi}_L \omega \Psi_R^3) + \bar{\lambda} \text{Tr} (\bar{\Xi}_L \omega^* \Psi_R^3) \quad (2.9) \\
 & + \sum_{a \in \{1,15\}} \left[\kappa_a \text{Tr} (\bar{\Psi}_L^l \mathcal{H}_a \Xi_R) + \bar{\kappa}_a \text{Tr} (\bar{\Psi}_L^l \mathcal{H}_a^* \Xi_R) \right] + \text{h.c.}
 \end{aligned}$$

All the coefficients of these fundamental Yukawa interactions, namely

$$\{y_a^l, \bar{y}_a^l, y_a^3, \bar{y}_a^3, \lambda, \bar{\lambda}, \kappa_a, \bar{\kappa}_a\}, \quad (2.10)$$

are presumed to be independent $\mathcal{O}(1)$ numbers.⁵

The model will explain the structure of fermion masses and mixings, while also producing third-family aligned U_1 leptoquarks that offer the best combined explanation of the B -physics anomalies, by breaking this large gauge symmetry down to the SM in a number of stages. The symmetry breaking pattern in this model is shown in figure 1. We do not attempt to explain the pattern of neutrino masses and mixings in this paper, although it is reasonable to suppose that a form of see-saw mechanism can deliver very light neutrinos. We postpone a detailed study of the neutrino sector for future work.

⁵The term in (2.9) with coupling $\bar{\lambda}$ will not in fact appear in the final formulae we obtain for the physical fermion mixing angles — but we include it here for completeness.

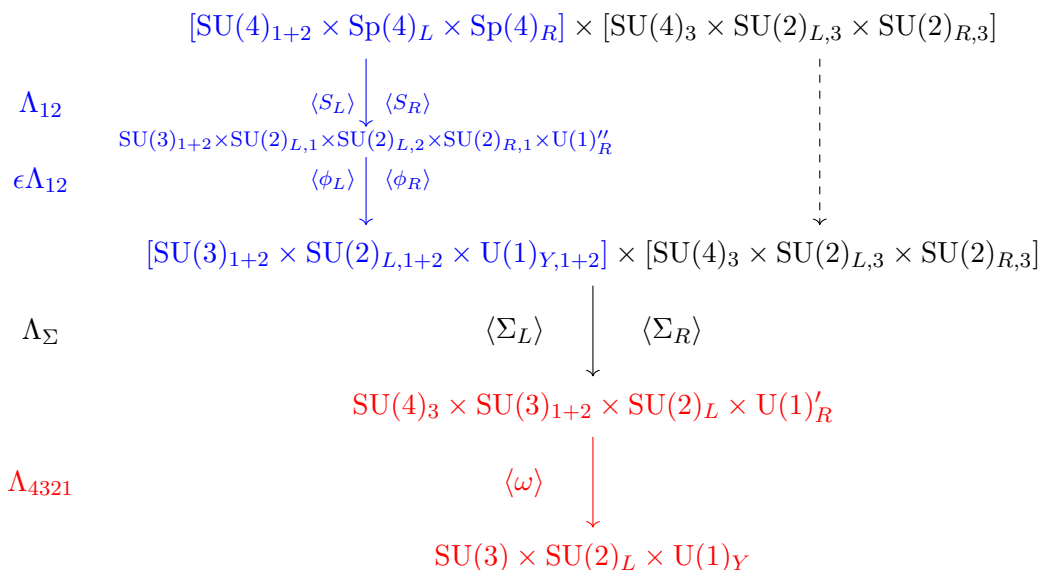


Figure 1. The symmetry breaking scheme in our model. The portion of the diagram coloured **blue** is responsible for generating the light family Yukawas, and thus for controlling the flavour structure of the light family sector. The portion coloured **red** mimics the low-energy breaking of so-called ‘4321 models’, delivering in particular a U_1 leptoquark coupled mostly to the third family. We will eventually suggest concrete scales for each Λ that appears on the vertical ‘axis’ — see figure 6.

3 Dynamical generation of the Yukawa sector

3.1 Electroweak light-flavour unification

In the 1–2 sector, we use electroweak flavour unification (EWFU) and its structured breaking to generate hierarchies in the Yukawa textures that can accommodate the data. (These symmetry breaking steps are coloured **blue** in figure 1.) This is a simplified, 2-family version of the mechanism that was first proposed in ref. [18] (see also [24]).

As in ref. [18], the idea is to first ‘deconstruct’ the flavour-unified gauge symmetry at a high scale using a pair of scalars transforming in the representations $S_L \sim (\mathbf{1}, \mathbf{5}, \mathbf{1})$ and $S_R \sim (\bar{\mathbf{4}}, \mathbf{1}, \mathbf{4})$ of G_{12} , before using scalars Φ_L and Φ_R in 2-index antisymmetrized representations (of $\text{Sp}(4)_L$ and $\text{Sp}(4)_R$ respectively) to ‘link’ the deconstructed gauge factors. In a little more detail, the key steps in the mechanism can be summarized as follows.

3.1.1 Sequential symmetry breaking (part I)

A. Deconstruction of electroweak symmetry, at scale Λ_{12} . First, the gauge-flavour unified symmetry is ‘deconstructed’ around a high scale Λ_{12} , which is so labelled because it is the scale at which the structure of the light-family Yukawa couplings are generated. This is done via a pair of scalars transforming in the representations $S_L \sim (\mathbf{1}, \mathbf{5}, \mathbf{1})$ and $S_R \sim (\bar{\mathbf{4}}, \mathbf{1}, \mathbf{4})$ of G_{12} . Explicitly, the breaking pattern is

$$\langle S_L \rangle : \text{Sp}(4)_L \longrightarrow \text{SU}(2)_{L,1} \times \text{SU}(2)_{L,2}, \quad (3.1)$$

$$\langle S_R \rangle : \text{SU}(4)_{1+2} \times \text{Sp}(4)_R \longrightarrow \text{SU}(3)_{1+2} \times \text{SU}(2)_{R,1} \times \text{U}(1)''_R, \quad (3.2)$$

where $U(1)''_R$ acts as $B - L$ on the right-handed first family, and as hypercharge on all other light fermions. This breaking can be achieved using vevs⁶

$$\langle S_L \rangle = \alpha_L \Lambda_{12} \begin{pmatrix} 0 & 0 & 1 & 0 \\ 0 & 0 & 0 & -1 \\ -1 & 0 & 0 & 0 \\ 0 & 1 & 0 & 0 \end{pmatrix}, \quad \langle S_R \rangle = \alpha_R \Lambda_{12} \begin{pmatrix} 0 & 0 & 0 & 0 \\ 0 & 0 & 0 & 0 \\ 0 & 0 & 0 & 0 \\ 0 & 1 & 0 & 0 \end{pmatrix} \quad (3.3)$$

where α_L and α_R are dimensionless numbers (that allow for the symmetry breaking in the left- and right-sectors to occur at slightly different scales, in the vicinity of Λ_{12}). Here, the vev of S_L , which transforms in an antisymmetrized 2-index representation of $Sp(4)_L$, is written as a 4-by-4 antisymmetric matrix. More precisely, the vev can be written (using the basis defined in section 2.1) as $\langle S_L \rangle = \alpha_L \Lambda_{12} (b_1 \wedge b_3 - b_2 \wedge b_4)$, where the wedge symbol ‘ \wedge ’ denotes antisymmetrization. The vev of S_R , which transforms in the $(\bar{4}, 4)$ representation of $SU(4) \times Sp(4)_R$, is written as a 4-by-4 matrix; in index notation, we have $\langle S_R \rangle = \alpha_R \Lambda_{12} a_4^* \otimes c_2$.

B. Integrate out heavy Higgs fields. Under the above deconstruction step, each of the Higgs fields $\mathcal{H}_1 \sim (\mathbf{1}, \mathbf{4}, \mathbf{4})$ and $\mathcal{H}_{15} \sim (\mathbf{15}, \mathbf{4}, \mathbf{4})$ decomposes into a set of ‘flavoured’ Higgs fields, with components coupling to each pair of light families (one left-handed, and one right-handed).⁷ Specifically, the $Sp(4)_L \times Sp(4)_R$ bifundamental representation $(\mathbf{4}, \mathbf{4})$ decomposes under Step 1, which breaks $SU(4)_{1+2} \times Sp(4)_L \times Sp(4)_R \rightarrow SU(3)_{1+2} \times SU(2)_{L,1} \times SU(2)_{L,2} \times SU(2)_{R,1} \times U(1)''_R$, as

$$\mathcal{H}_a \sim (\mathbf{4}, \mathbf{4})_a \mapsto \underbrace{(\mathbf{2}, \mathbf{1}, \mathbf{2})_0}_{\mathcal{H}_a^{11}} \oplus \underbrace{(\mathbf{1}, \mathbf{2}, \mathbf{2})_0}_{\mathcal{H}_a^{21}} \oplus \underbrace{(\mathbf{2}, \mathbf{1}, \mathbf{1})_{\frac{1}{2}}}_{\mathcal{H}_a^{12+}} \oplus \underbrace{(\mathbf{2}, \mathbf{1}, \mathbf{1})_{-\frac{1}{2}}}_{\mathcal{H}_a^{12-}} \oplus \underbrace{(\mathbf{1}, \mathbf{2}, \mathbf{1})_{\frac{1}{2}}}_{\mathcal{H}_a^{22+}} \oplus \underbrace{(\mathbf{1}, \mathbf{2}, \mathbf{1})_{-\frac{1}{2}}}_{\mathcal{H}_a^{22-}}, \quad (3.4)$$

where we use the notation \mathcal{H}_a^{ij} to denote an $SU(3)_{1+2}$ singlet component coming from \mathcal{H}_a , that couples to the i^{th} generation of left-handed fermion, and the j^{th} generation of right-handed fermion.⁸ It is assumed that most of these flavoured Higgs components are heavy, except for the $\mathcal{H}_a^{22\pm}$ components which we suppose are lighter, and which will ultimately mix with the physical Higgses (see section 4). It is this presumed structure of the quadratic Higgs mass terms that *defines* the second generation; modulo these scalar mass terms, the theory is at this point still invariant under permuting the family labels of left-handed light fermions.

⁶The fact that the vev of $S_L \sim \mathbf{5}$ deconstructs $Sp(4)_L \rightarrow SU(2)_{L,1} \times SU(2)_{L,2}$ is easily understood at the Lie algebra level by recalling that $\mathfrak{sp}(4) \cong \mathfrak{so}(5)$. The field $S_L \sim \mathbf{5}$ transforms in the fundamental vector representation of $\mathfrak{so}(5)$, and so a generic vev breaks $\mathfrak{so}(5)$ to an $\mathfrak{so}(4) \cong \mathfrak{su}(2) \oplus \mathfrak{su}(2)$ subalgebra. At the group level, this translates to the breaking $Sp(4) \rightarrow SU(2) \times SU(2)$. It is straightforward to show that the vev direction (3.3) breaks $Sp(4)$ to the particular $SU(2)_{L,1} \times SU(2)_{L,2}$ subgroup that we want to preserve.

⁷This kind of model-building structure, whereby a generic set of flavoured Higgs fields are ultimately responsible for generating hierarchies in the Yukawa couplings, is reminiscent of the ‘scalar democracy’ idea proposed in refs. [25, 26]. Electroweak-flavour unification is a natural UV framework for realising scalar democracy.

⁸The notation \mathcal{H}_{15}^{ij} therefore denotes an $SU(3)_{1+2}$ singlet components originating from the decomposition of the adjoint Higgs \mathcal{H}_{15} .

Concretely, denoting with M_a^{ij} the mass of field $\mathcal{H}_a^{ij(\pm)}$, we assume the scalar potential is such that

$$M_a^{11} \approx M_a^{12} \approx M_a^{21} \approx \Lambda_{12}, \quad (3.5)$$

$$M_a^{22} \text{ somewhat lighter.} \quad (3.6)$$

The heavy components are all integrated out at the scale Λ_{12} . This generates many EFT couplings, including higher-dimensional Yukawa operators that couple the remaining dynamical Higgs fields \mathcal{H}_a^{22} (which will mix with the physical Higgs) to the first generation fermions. At the level of the EFT, one can already see that gauge invariance requires one insertion of Φ_L (Φ_R) to couple \mathcal{H}_a^{22} to a left-handed (right-handed) first generation fermion. Thus, schematically, the effective Yukawa couplings have the form

$$\mathcal{L}_{\text{EFT}} \supset \bar{f}_{L,2} \mathcal{H}_a^{22} f_{R,2} + \frac{\Phi_L}{\Lambda_{12}} \bar{f}_{L,1} \mathcal{H}_a^{22} f_{R,2} + \frac{\Phi_R}{\Lambda_{12}} \bar{f}_{L,2} \mathcal{H}_a^{22} f_{R,1} + \frac{\Phi_L \Phi_R}{\Lambda_{12}^2} \bar{f}_{L,1} \mathcal{H}_a^{22} f_{R,1}, \quad (3.7)$$

for each fermion type $f \in \{u, d, e\}$. We give the precise expressions in eqs. (3.14)–(3.20).

C. Break to the (light-flavour) SM, at scales $\epsilon_{L,R} \Lambda_{12}$. Finally, there are the remaining dynamical scalars Φ_L (real) and Φ_R (complex), which are in 2-index antisymmetrized representations (the **5**) of $\text{Sp}(4)_L$ and $\text{Sp}(4)_R$ respectively that can be represented by antisymmetric 4-by-4 matrices. These scalar fields acquire vevs to ‘link’ the deconstructed gauge factors. The required vevs are embedded as

$$\langle \Phi_L \rangle = \Lambda_{12} \epsilon_L \begin{pmatrix} 0 & 0 & 0 & 1 \\ 0 & 0 & 1 & 0 \\ 0 & -1 & 0 & 0 \\ -1 & 0 & 0 & 0 \end{pmatrix}, \quad \langle \Phi_R \rangle = \Lambda_{12} \epsilon_R \begin{pmatrix} 0 & 0 & 0 & z_+ \\ 0 & 0 & z_- & 0 \\ 0 & -z_- & 0 & 0 \\ -z_+ & 0 & 0 & 0 \end{pmatrix}, \quad (3.8)$$

where z_{\pm} are (independent) dimensionless, order-1 \mathbb{C} -numbers. In our index notation these vevs are

$$\langle \Phi_L \rangle = \Lambda_{12} \epsilon_L (b_1 \wedge b_4 + b_2 \wedge b_3) =: \langle \phi_L \rangle, \quad (3.9)$$

$$\langle \Phi_R \rangle = \underbrace{\Lambda_{12} \epsilon_R z_+ c_1 \wedge c_4}_{\langle \phi_{R+} \rangle} + \underbrace{\Lambda_{12} \epsilon_R z_- c_2 \wedge c_3}_{\langle \phi_{R-} \rangle} \quad (3.10)$$

where, in the second line, it is convenient to identify specific components of $\Phi_{L,R}$ with distinct link fields ϕ_L , ϕ_{R+} and ϕ_{R-} in the broken phase. These transform in the representations $\phi_L \sim (\mathbf{2}, \mathbf{2})$ of $\text{SU}(2)_{L,1} \times \text{SU}(2)_{L,2}$, and $\phi_{R\pm} \sim \mathbf{2}_{\pm \frac{1}{2}}$ of $\text{SU}(2)_{R,1} \times \text{U}(1)''_R$. The factors ϵ_L and ϵ_R are small, \mathbb{R} -valued parameters, which parametrize the ratios of energy scales between the $\Phi_{L,R}$ condensation scale and the heavier scale Λ_{12} at which the heavy Higgs components are integrated out.

These vevs trigger the symmetry breaking

$$\langle \Phi_L \rangle : \text{SU}(2)_{L,1} \times \text{SU}(2)_{L,2} \longrightarrow \text{SU}(2)_{L,1+2}, \quad (3.11)$$

$$\langle \Phi_R \rangle : \text{SU}(2)_{R,1} \times \text{U}(1)''_R \longrightarrow \text{U}(1)_{Y,1+2}, \quad (3.12)$$

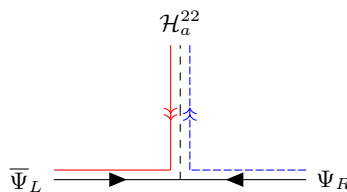


Figure 2. Feynman diagram representing the direct coupling of second generation fermions to the \mathcal{H}_a^{22} Higgs components, which ultimately mix with the H_a fields and result in the 2–2 Yukawa couplings.

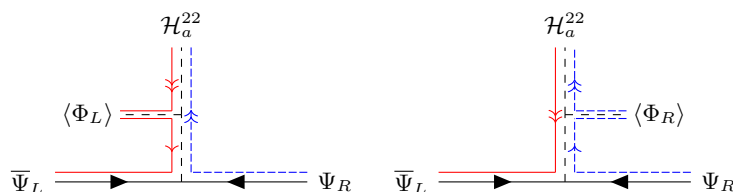


Figure 3. Feynman diagrams that contribute to the 1–2 (left) and 2–1 (right) elements of the Yukawa matrices, once the heavy Higgs components running along the internal lines are integrated out at Λ_{12} .

the result of which is $SM_{1+2} := SU(3)_{1+2} \times SU(2)_{L,1+2} \times U(1)_{Y,1+2}$, the (light-flavour) SM gauge symmetry. Once this condensation of Φ_L and Φ_R occurs, the EFT Yukawa operators generated in Step B match onto dimension-4 Yukawa couplings of the first generation fermions to the field \mathcal{H}_a^{22} , with in-built EFT suppression factors of ϵ_L and $\epsilon_{R\pm}$.

3.1.2 EFT matching for light Yukawas

Having described the essential elements of the EWFU mechanism for generating Yukawa hierarchies, which we here adapt from ref. [18] to the 2-flavour sector, we now give the details of the EFT matching.

The effective Yukawa operators that we wrote schematically in eq. (3.7) are automatically generated upon integrating out the heavy components of \mathcal{H}_a^{ij} at scale Λ_{12} , provided the UV model contains the following gauge invariant cubic and quartic scalar interactions

$$\begin{aligned}
 V(\Phi, H) \supset & \sum_{a \in \{1,15\}} \Lambda_{12} [\beta_L^a \text{Tr} (\mathcal{H}_a^* \Phi_L \mathcal{H}_a) + \beta_R^a \text{Tr} (\mathcal{H}_a^* \mathcal{H}_a \Phi_R) + \beta_R^{a*} \text{Tr} (\mathcal{H}_a^* \mathcal{H}_a \Phi_R^*)] \\
 & + \sum_{a \in \{1,15\}} \beta_{LR}^a \text{Tr} (\mathcal{H}_a^* \Phi_L \mathcal{H}_a \Phi_R) + \beta_{LR}^{a*} \text{Tr} (\mathcal{H}_a^* \Phi_L \mathcal{H}_a \Phi_R^*), \tag{3.13}
 \end{aligned}$$

which couple the \mathcal{H}_a Higgs fields (and their conjugates) to the symmetry breaking scalars Φ_L and Φ_R . Given these scalar interactions, one can draw the Feynman diagrams shown in figures 2–4; upon integrating out the \mathcal{H}_a^{ij} components, which run as internal propagators, one gets the desired higher-dimension Yukawa operators.

If we decompose the fermion fields into their family-deconstructed components, i.e. those states relevant after all the symmetry breaking steps detailed in section 3.1, the resulting

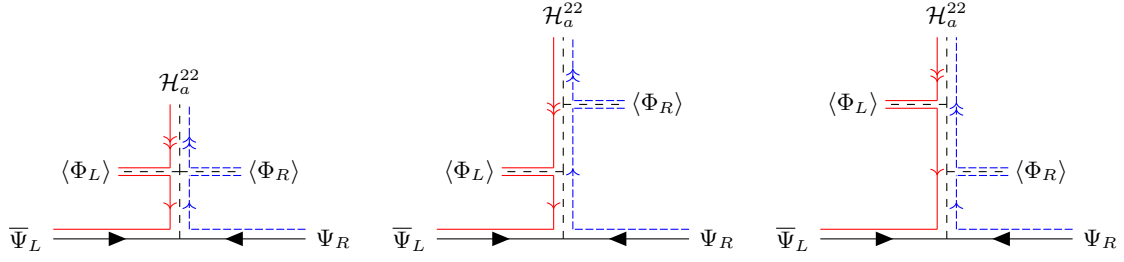


Figure 4. Feynman diagrams that contribute to the 1–1 element of the Yukawa matrices, once the heavy Higgs components running along the internal lines are integrated out at Λ_{12} . The presence of the diagram on the left is essential in order to provide enough freedom to parametrize the 1–1 entry independently of the 1–2 and 2–1 entries.

effective Yukawa operators obtained by EFT matching can be organised by increasing mass dimension, as follows.

Dimension 4 (see figure 2):

$$\begin{aligned}
 \mathcal{L}_{\text{EFT}} \supset & \bar{Q}_{L,2} \left(y_1^l \mathcal{H}_1^{22-} + \bar{y}_1^l \mathcal{H}_1^{22+*} + y_{15}^l \mathcal{H}_{15}^{22-} + \bar{y}_{15}^l \mathcal{H}_{15}^{22+*} \right) u_{R,2} + \text{h.c.} \\
 & + \bar{Q}_{L,2} \left(y_1^l \mathcal{H}_1^{22+} + \bar{y}_1^l \mathcal{H}_1^{22-*} + y_{15}^l \mathcal{H}_{15}^{22+} + \bar{y}_{15}^l \mathcal{H}_{15}^{22-*} \right) d_{R,2} + \text{h.c.} \\
 & + \bar{L}_{L,2} \left(y_1^l \mathcal{H}_1^{22+} + \bar{y}_1^l \mathcal{H}_1^{22-*} - 3y_{15}^l \mathcal{H}_{15}^{22+} - 3\bar{y}_{15}^l \mathcal{H}_{15}^{22-*} \right) e_{R,2} + \text{h.c.} . \quad (3.14)
 \end{aligned}$$

To simplify the notation, it is convenient to define:

$$\begin{pmatrix} \mathcal{H}_a^u \\ \bar{\mathcal{H}}_a^u \end{pmatrix} = \mathcal{R}_a \begin{pmatrix} \mathcal{H}_a^{22-} \\ \mathcal{H}_a^{22+*} \end{pmatrix}, \quad \begin{pmatrix} \mathcal{H}_a^d \\ \bar{\mathcal{H}}_a^d \end{pmatrix} = \mathcal{R}_a \begin{pmatrix} \mathcal{H}_a^{22+} \\ \mathcal{H}_a^{22-*} \end{pmatrix}, \quad (3.15)$$

where the unitary matrix \mathcal{R}_a is

$$\mathcal{R}_a = \frac{1}{\sqrt{|y_a^l|^2 + |\bar{y}_a^l|^2}} \begin{pmatrix} y_a^l & \bar{y}_a^l \\ -(\bar{y}_a^l)^* & (y_a^l)^* \end{pmatrix}. \quad (3.16)$$

This way only the combinations $\mathcal{H}_a^{u,d}$ appear in the Yukawa interaction (3.14). The latter assumes the simple form

$$\mathcal{L}_{\text{EFT}} \supset \sum_{a \in \{1,15\}} \tilde{y}_a^l \left(\bar{Q}_{L,2} \mathcal{H}_a^u u_{R,2} + \bar{Q}_{L,2} \mathcal{H}_a^d d_{R,2} + \bar{L}_{L,2} \Gamma_a \mathcal{H}_a^d e_{R,2} \right) + \text{h.c.}, \quad (3.17)$$

where $\Gamma_1 \equiv 1$ and $\Gamma_{15} \equiv -3$ encode the different treatment of the SU(3)-singlet piece (i.e. the leptons) contained in SU(4), and

$$\tilde{y}_a^l = \sqrt{|y_a^l|^2 + |\bar{y}_a^l|^2}. \quad (3.18)$$

Proceeding in a similar manner, the subleading contributions to the effective Yukawa interaction generated by high-dimensional operators are as follows.

Dimension 5 (see figure 3):

$$\begin{aligned}
 \mathcal{L}_{\text{EFT}} \supset \sum_{a \in \{1,15\}} \tilde{y}_a^l & \left[\bar{u}_{L,1} \frac{\beta_L^a \phi_L}{\Lambda_{12}} \mathcal{H}_a^u u_{R,2} + \bar{u}_{L,2} \left(\frac{\beta_R^a \phi_{R+}}{\Lambda_{12}} + \frac{\beta_R^{a*} \phi_{R-}^*}{\Lambda_{12}} \right) \mathcal{H}_a^u u_{R,1} \right. \\
 & + \bar{d}_{L,1} \frac{\beta_L^a \phi_L}{\Lambda_{12}} \mathcal{H}_a^d d_{R,2} + \bar{d}_{L,2} \left(\frac{\beta_R^a \phi_{R+}}{\Lambda_{12}} + \frac{\beta_R^{a*} \phi_{R-}^*}{\Lambda_{12}} \right) \mathcal{H}_a^d d_{R,1} \\
 & \left. + (d \leftrightarrow e, \tilde{y}_a^l \leftrightarrow \Gamma_a \tilde{y}_a^l) \right] + \text{h.c.} .
 \end{aligned} \tag{3.19}$$

Dimension 6 (see figure 4):

$$\begin{aligned}
 \mathcal{L}_{\text{EFT}} \supset \sum_{a \in \{1,15\}} \tilde{y}_a^l & \left[\bar{u}_{L,1} \left(\frac{(\beta_{LR}^a + 2\beta_L^a \beta_R^a) \phi_L \phi_{R+}}{\Lambda_{12}^2} + \frac{(\beta_{LR}^{a*} + 2\beta_L^a \beta_R^{a*}) \phi_L \phi_{R-}^*}{\Lambda_{12}^2} \right) \mathcal{H}_a^u u_{R,1} \right. \\
 & + \bar{d}_{L,1} \left(\frac{(\beta_{LR}^a + 2\beta_L^a \beta_R^a) \phi_L \phi_{R+}^*}{\Lambda_{12}^2} + \frac{(\beta_{LR}^{a*} + 2\beta_L^a \beta_R^{a*}) \phi_L \phi_{R-}}{\Lambda_{12}^2} \right) \mathcal{H}_a^d d_{R,1} \\
 & \left. + (d \leftrightarrow e, \tilde{y}_a^l \leftrightarrow \Gamma_a \tilde{y}_a^l) \right] + \text{h.c.} .
 \end{aligned} \tag{3.20}$$

To summarize the 1–2 sector generated by this mechanism, for all three types of SM fermion $f \in \{u, d, e\}$, the Yukawa couplings Y_f^{22} between the light families and the \mathcal{H}^{22} Higgs fields have the hierarchical structure

$$Y_f^{22} \sim \begin{pmatrix} \epsilon_L \epsilon_R & \epsilon_L \\ \epsilon_R & 1 \end{pmatrix}. \tag{3.21}$$

This is the 2-flavour version of the EWFU structure derived in [18].

3.2 Mixing with the third family

At this point the construction of the Yukawa sector departs from the EWFU mechanism of [18] (which essentially replicates the structure we have just described in all three families). For us, the third family is treated differently in the UV, coupling to its own decoupled Pati-Salam gauge factor G_3 , as in eqs. (2.1)–(2.2).

Before we explain how the remaining Yukawa couplings (that mix with the third family) are generated, we must explain the final symmetry breaking steps needed to take us from $\text{SM}_{1+2} \times G_3$ down to SM_{1+2+3} , the SM gauge symmetry. Continuing our labelling from that of section 3.1, these steps are the following.

3.2.1 Sequential symmetry breaking (part II)

D. Linking of electroweak symmetry, at scale Λ_Σ . The lowest breaking step (E) will, by design, mimic the symmetry breaking in so-called ‘4321 models’ [11, 12, 27]. To make contact with this requires we first link together the electroweak symmetries, which remain partially deconstructed. This step resembles a similar linking step in the ‘Pati-Salam cubed’ UV completion [5, 28, 29] of 4321. This breaking step is triggered by two complex scalar fields, which start life in representations $\Sigma_L \sim (\mathbf{1}, \mathbf{4}, \mathbf{1}) \otimes (\mathbf{1}, \mathbf{2}, \mathbf{1})$ and $\Sigma_R \sim (\mathbf{1}, \mathbf{1}, \mathbf{4}) \otimes (\mathbf{1}, \mathbf{1}, \mathbf{2})$ of the UV gauge symmetry G (2.1).

Representing both these bifundamentals as 2-by-4 matrices (for which each row transforms as an $\text{Sp}(4)_{L/R}$ fundamental), appropriate vevs are

$$\langle \Sigma_L \rangle = \gamma_L \Lambda_\Sigma \mathbf{M}, \quad \langle \Sigma_R \rangle = \gamma_R \Lambda_\Sigma \mathbf{M}, \quad (3.22)$$

where the matrix \mathbf{M} is

$$\mathbf{M} = \begin{pmatrix} 0 & 1 & 0 & 0 \\ 0 & 0 & 0 & 1 \end{pmatrix}. \quad (3.23)$$

In our index notation, this is equivalent to $\langle \Sigma_L \rangle = \gamma_L \Lambda_\Sigma (b_2 \otimes B_1 + b_4 \otimes B_2)$ and $\langle \Sigma_R \rangle = \gamma_R \Lambda_\Sigma (c_2 \otimes C_1 + c_4 \otimes C_2)$. The result is to break

$$\text{SU}(2)_{L,1+2} \times \text{U}(1)_{Y,1+2} \times \text{SU}(2)_{L,3} \times \text{SU}(2)_{R,3} \longrightarrow \text{SU}(2)_L \times \text{U}(1)'_R, \quad (3.24)$$

leaving the electroweak factor of the 4321 model. Here $\text{U}(1)'_R$ acts as hypercharge on the light families, and as $\text{U}(1)_R$ (i.e. the subgroup of $\text{SU}(2)_R$ generated by σ_3) on the third family.

As for Step C above, we can decompose these symmetry breaking scalars into components of the intermediate gauge symmetry that remains dynamical at this scale, namely $\text{SM}_{1+2} \times G_3$. The field Σ_L just splits into a pair of bidoublets,

$$\Sigma_L \longrightarrow (\mathbf{2}, \mathbf{2})^{\oplus 2} \quad \text{of} \quad \text{SU}(2)_{L,1+2} \times \text{SU}(2)_{L,3}, \quad (3.25)$$

while

$$\Sigma_R \longrightarrow (+1/2, \mathbf{2})^{\oplus 2} \oplus (-1/2, \mathbf{2})^{\oplus 2} \quad \text{of} \quad \text{U}(1)_{Y,1+2} \times \text{SU}(2)_{R,3}. \quad (3.26)$$

The fact that all the fields in these decompositions are duplicated is because of their origin in the gauge-flavour unified $\text{Sp}(4)_{L(R)}$ symmetries; there is *one copy* of every field *for each light family*. The vevs (3.22)–(3.23) sit in $\text{Sp}(4)$ components corresponding to the second family; while other choices would have achieved the same symmetry breaking pattern (which is obvious because the decompositions (3.25)–(3.26) carry no trace of the light family index, which has now been linked together in SM_{1+2}), we will see that the vevs of $\Sigma_{L,R}$ play another role. This second role is in the mixing of the different Higgs fields to produce the physical mass eigenstates; as we alluded to above, this is where the second and first family are distinguished, and so the choice (3.23) is important. See section 4.1.1.

E. Breaking 4321 to the Standard Model, at scale Λ_{4321} . At this point, the gauge symmetry is that of the 4321 model, namely

$$\text{SU}(4)_3 \times \text{SU}(3)_{1+2} \times \text{SU}(2)_L \times \text{U}(1)'_R. \quad (3.27)$$

Even though the gauge group (and its action on the SM chiral fermions) is the same as for established 4321 models [11, 12, 27], this model features a different scalar sector and choice of vector-like fermion, which we record in table 2.⁹

⁹Specifically concerning the vector-like fermions (VLFs), we here consider a VLF that is a singlet under all of G_3 , which means it decomposes to singlets under the $\text{SU}(4)_3$ factor of 4321 — this is a minimal choice for generating the required mixings in the Yukawa sector (as is explained in this section). In contrast, 4321 models designed to fit the central value of $R_{D^{(*)}}$ anomaly (see section 4.2.1) feature VLFs charged under $\text{SU}(4)_3$, which are required to modify the flavour structure of the U_1 leptoquark to fit the anomaly (without contravening high- p_T bounds). For a phenomenological analysis including recent data, see [30].

	Field ($i, j = 1, 2$)	$SU(4)_3$	$SU(3)_{1+2}$	$SU(2)_L$	$U(1)'_R$
SM Fermions (chiral)	Q_L^i	1	3	2	1/6
	u_R^i	1	3	1	2/3
	d_R^i	1	3	1	-1/3
	L_L^i	1	3	2	-1/2
	e_R^i	1	3	1	-1
	ν_R^i	1	3	1	0
	Ψ_L^3	4	1	2	0
	$\Psi_{R,u}^3$	4	1	1	1/2
	$\Psi_{R,d}^3$	4	1	1	-1/2
Vector-like fermion	ξ_u^i	1	3	1	2/3
	ξ_d^i	1	3	1	-1/3
	ξ_e^i	1	1	1	-1
	ξ_ν^i	1	1	1	0
Higgses (light only)	\mathcal{H}_a^{22+}	1	1	2	+1/2
	\mathcal{H}_a^{22-}	1	1	2	-1/2
	R_2	1	3	2	7/6
	\tilde{R}_2	1	3	2	1/6
	H_1^+	1	1	2	1/2
	H_{15}^+	15	1	2	1/2
	H_1^-	1	1	2	-1/2
	H_{15}^-	15	1	2	-1/2
Symmetry breaking scalars	ω_{uu}^{i3}	$\bar{\mathbf{4}}$	3	1	7/6
	$\omega_{ud}^{i3}, \omega_{ud}^{3i}$	$\bar{\mathbf{4}}$	3	1	1/6
	ω_{dd}^{i3}	$\bar{\mathbf{4}}$	3	1	-5/6
	$\omega_{\nu\nu}^{i3}$	$\bar{\mathbf{4}}$	1	1	1/2
	$\omega_{e\nu}^{i3}, \omega_{\nu e}^{3i}$	$\bar{\mathbf{4}}$	1	1	-1/2
	ω_{ee}^{i3}	$\bar{\mathbf{4}}$	1	1	-3/2

Table 2. Field content of the model before 4321 breaking. Of the scalar fields (listed in the last two blocks), those that acquire non-vanishing vevs are indicated by grey shading.

The remaining symmetry breaking step is to the SM. The final scalar field ω , whose vev triggers this breaking, transforms in the representation $\omega \sim (\mathbf{4}, \mathbf{1}, \mathbf{4}) \otimes (\bar{\mathbf{4}}, \mathbf{1}, \mathbf{2})$ of the UV gauge symmetry G (2.1). At this point it is not so enlightening to record how the vev is embedded in the UV field, so we begin by decomposing this field under the 4321 group (3.27). We have¹⁰

$$\begin{aligned}
 \omega &\rightarrow \hat{\omega}_3 \oplus \hat{\omega}_1, & (3.28) \\
 \hat{\omega}_3 &\sim \underbrace{\{(\bar{\mathbf{4}}, \mathbf{3}, \mathbf{1}, 7/6) \oplus (\bar{\mathbf{4}}, \mathbf{3}, \mathbf{1}, 1/6)\}^{\oplus 2}}_{\omega_{uu}^{i3}} \oplus \underbrace{\{(\bar{\mathbf{4}}, \mathbf{3}, \mathbf{1}, -5/6)\}^{\oplus 2}}_{\omega_{ud}^{i3}, \omega_{ud}^{3i}} \oplus \underbrace{\{(\bar{\mathbf{4}}, \mathbf{3}, \mathbf{1}, -5/6)\}^{\oplus 2}}_{\omega_{dd}^{i3}}, \\
 \hat{\omega}_1 &\sim \underbrace{\{(\bar{\mathbf{4}}, \mathbf{1}, \mathbf{1}, 1/2) \oplus (\bar{\mathbf{4}}, \mathbf{1}, \mathbf{1}, -1/2)\}^{\oplus 2}}_{\omega_{\nu\nu}^{i3}} \oplus \underbrace{\{(\bar{\mathbf{4}}, \mathbf{1}, \mathbf{1}, -3/2)\}^{\oplus 2}}_{\omega_{\nu e}^{i3}, \omega_{\nu e}^{3i}} \oplus \underbrace{\{(\bar{\mathbf{4}}, \mathbf{1}, \mathbf{1}, -3/2)\}^{\oplus 2}}_{\omega_{ee}^{i3}}.
 \end{aligned}$$

¹⁰Note that the fields here labelled $\hat{\omega}_{3(1)}$ themselves denote *reducible* representations of 4321, which we use as a notational convenience to gather together the $SU(3)_{1+2}$ triplets (singlets).

Our notation here needs a little explanation. The subscript label indicates the pair of fermion types to which that ω component couples; for example, the fields ω_{uu}^{i3} are colour triplets and so couple to di-quark pairs, and their $U(1)'_R$ charge of $+7/6$ means they couple specifically to pairs of up-type quarks. The superscript label then indicates the family indices of the fermion pair to which that ω component couples. One of these is always a third family label, and the other is always a light family label which can run over $i \in \{1, 2\}$; this is because the UV field ω is in a bifundamental representation of $Sp(4)_{R,12} \times SU(2)_{R,3}$, and the duplication labelled by i comes from the fact that $Sp(4)_{R,12}$ stores a light family index. For the fields with ‘mixed couplings’, i.e. to one up-type and one down-type quark, there is a further duplication due to the fact that there are components coupling to {second family down-type, third family up-type}, and vice-versa. Thus, for example, there are four of these scalars with quantum numbers $(\bar{\mathbf{4}}, \mathbf{3}, \mathbf{1}, 1/6)$. To emphasize this, we will at times use notation

$$\omega_{ud}^{13} \equiv \omega^{ub}, \quad \omega_{ud}^{23} \equiv \omega^{cb}, \quad \omega_{ud}^{31} \equiv \omega^{td}, \quad \omega_{ud}^{32} \equiv \omega^{ts}, \quad (3.29)$$

labelling the quark (or lepton) flavours explicitly.

The 4321 gauge symmetry is broken down to the SM gauge symmetry, i.e.

$$SU(4)_3 \times SU(3)_{1+2} \times SU(2)_L \times U(1)'_R \longrightarrow SU(3) \times SU(2)_L \times U(1)_Y, \quad (3.30)$$

if any of the components $\omega_{ud}^{i3,3i}$ (and possibly $\omega_{\nu e}^{i3,3i}$) acquire non-zero vevs in the directions

$$\langle \omega_{ud}^{i3,3i} \rangle = \frac{v_3}{\sqrt{2}} \begin{pmatrix} 1 & 0 & 0 \\ 0 & 1 & 0 \\ 0 & 0 & 1 \\ 0 & 0 & 0 \end{pmatrix}, \quad \langle \omega_{\nu e}^{i3,3i} \rangle = \frac{v_1}{\sqrt{2}} \begin{pmatrix} 0 \\ 0 \\ 0 \\ 1 \end{pmatrix}, \quad (3.31)$$

mimicking the original 4321 setup of [11], where we represent $\omega_{ud}^{i3,3i}$ and $\omega_{\nu e}^{i3,3i}$ as a 4-by-3 matrix and a 4-vector respectively.

However, as a point of departure from other 4321 models in the literature, we emphasize that in this model there are four copies of each of these scalars, as listed in (3.29). Which of these copies acquire symmetry-breaking vevs in fact has physical consequences; after integrating out the vector-like fermion (VLF) Ξ (see the following section 3.2.2), the choice of vev-acquiring- ω fields determines which 2–3 Yukawa elements are populated in our EFT (up to subleading corrections due to mixing effects between the scalars). While all choices are equally natural, phenomenological reasons suggest we take the components

$$\omega_{ud}^{23} \equiv \omega^{cb} \quad \text{and} \quad \omega_{\nu e}^{32} \equiv \omega^{\nu\tau\mu} \quad (3.32)$$

as the (only) ones that get the vevs indicated in eq. (3.31).

3.2.2 EFT matching for third family Yukawas and mixings

Another ingredient is required to generate mixing between the light families and the third, and this is the vector-like fermion (VLF) $\Xi \sim (\mathbf{4}, \mathbf{1}, \mathbf{4}) \otimes (\mathbf{1}, \mathbf{1}, \mathbf{1})$, which has the same quantum numbers as the field Ψ^l_R .

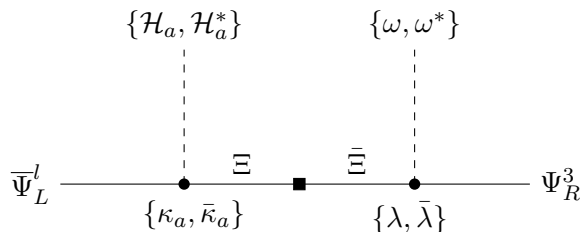


Figure 5. Feynman diagrams, depicted in the unbroken $G_{12} \times G_3$ phase, that lead to mixing between the third family and light family fermions. Integrating out the VLF Ξ and expanding the scalar field ω about its vev gives the relevant effective Yukawa couplings mixing the light families with the third. The notation ‘ $\{\kappa, \bar{\kappa}\}$ ’ denotes, for example, that there are two possible couplings that can feature, connecting to either \mathcal{H}_a or its conjugate \mathcal{H}^* . Recall from section 2.3 that the bar denotes an independent coupling.

This VLF permits the fundamental Yukawa interactions written above in eq. (2.9), which *link* third family fermion fields to the light fermions via either $\mathcal{H}_a^{(*)}$ or ω . Using these interactions, one can write down the Feynman diagram in figure 5, that links Ψ_L^l with Ψ_R^3 . Note that, given the quantum numbers of the fields in our model (in particular, given the quantum numbers of Ξ), there is no corresponding tree-level diagram by which we can link Ψ_L^3 with Ψ_R^l .¹¹

Since the fields \mathcal{H}_a will mix with the physical Higgs (through the components $\mathcal{H}_a^{22\pm}$ introduced in (3.4)), the Feynman diagram in figure 5 will result in Yukawa couplings linking light left-handed fermions with the third family right-handed fields, populating the third column (but not the third row) of the Yukawa matrices. These terms will moreover be suppressed (with respect to the 33 entries of the Yukawa matrices) by the same overall factor by which the second family masses are suppressed, helping to explain why the mixing angles with the third family are so small.¹²

Under 4321 the VLF decomposes as

$$\begin{aligned} \Xi &\rightarrow \hat{\xi}_3 \oplus \hat{\xi}_1, & (3.33) \\ \hat{\xi}_3 &\sim \underbrace{\{(1, \mathbf{3}, 1, 2/3)\}}_{\xi_u^i} \oplus \underbrace{\{(1, \mathbf{3}, 1, -1/3)\}}_{\xi_d^i}^{\oplus 2}, \\ \hat{\xi}_1 &\sim \underbrace{\{(1, \mathbf{1}, 1, 0)\}}_{\xi_\nu^i} \oplus \underbrace{\{(1, \mathbf{1}, 1, -1)\}}_{\xi_e^i}^{\oplus 2}, \end{aligned}$$

where we employ a similar notation to that used for ω in (3.28). Again, there are two copies of each 4321 representation; one set of VLFs couples to the first family fermions, and the

¹¹Such terms, which would populate the third row of the Yukawa matrices, would be generated if we further added a VLF charged under $\text{Sp}(4)_L$, which we choose not to.

¹²If we had instead included a VLF charged under G_3 , the 1–3 and 2–3 entries of the Yukawa matrices would be populated by direct couplings to the H_1 and H_{15} Higgs fields, which recall are those Higgses charged under G_3 . This is a less desirable option, because the smallness of the 1–3 and 2–3 quark mixing angles would have to be explained purely as a result of the heaviness of the VLF with respect to $v_{1,3}$.

other set to the second family, and this is labelled by the index i , coloured **red**. Both sets of interactions are present in the UV couplings (2.9).

In the 4321 phase, the diagram in figure 5 decomposes into separate contributions (with different mediator fields) for quarks and leptons. The $SU(3)_{1+2}$ triplet components $(\omega_{ud}, \xi_{u,d}^2)$ contribute to the quark Yukawas, while the $SU(3)_{1+2}$ singlets $(\omega_{\nu e}, \xi_{\nu,e}^2)$ contribute to the lepton Yukawas.

Similarly to the case of the light Yukawa couplings, it is convenient to introduce a new Higgs basis

$$\begin{pmatrix} (\mathcal{H}_\kappa)_a^u \\ (\overline{\mathcal{H}}_\kappa)_a^u \end{pmatrix} = \mathcal{K}_a \begin{pmatrix} \mathcal{H}_a^{22-} \\ \mathcal{H}_a^{22+*} \end{pmatrix}, \quad \begin{pmatrix} (\mathcal{H}_\kappa)_a^d \\ (\overline{\mathcal{H}}_\kappa)_a^d \end{pmatrix} := \mathcal{K}_a \begin{pmatrix} \mathcal{H}_a^{22+} \\ \mathcal{H}_a^{22-*} \end{pmatrix}, \quad (3.34)$$

where

$$\mathcal{K}_a := \frac{1}{\sqrt{|\kappa_a|^2 + |\bar{\kappa}_a|^2}} \begin{pmatrix} \kappa_a & \bar{\kappa}_a \\ -(\bar{\kappa}_a)^* & (\kappa_a)^* \end{pmatrix}. \quad (3.35)$$

Defining in addition

$$\tilde{\kappa}_a = \sqrt{|\kappa_a|^2 + |\bar{\kappa}_a|^2}, \quad (3.36)$$

the effective heavy-light Yukawa interactions assume the form

$$\mathcal{L} \supset \sum_{a \in \{1,15\}} \frac{\lambda v_3 \tilde{\kappa}_a}{m \xi_u^2} [\bar{u}_{L,2} (\mathcal{H}_\kappa)_a^u u_{R,3} + \beta_L^a \epsilon_L \bar{u}_{L,1} (\mathcal{H}_\kappa)_a^u u_{R,3}] \quad (3.37)$$

$$+ \frac{\lambda v_1 \tilde{\kappa}_a}{m \xi_e^2} [\bar{e}_{L,2} (\mathcal{H}_\kappa)_a^d e_{R,3} + \beta_L^a \epsilon_L \bar{e}_{L,1} (\mathcal{H}_\kappa)_a^d e_{R,3}] + \text{h.c.} \quad (3.38)$$

We remark that there is no equivalent mixing term generated in the down-quark sector, at least to this order, because of the 4321-breaking vev appearing in the ω^{cb} component, as in eq. (3.32). It turns out that the vertex with coupling $\bar{\lambda}$, defined in the UV Lagrangian (2.9), does not contribute to any non-vanishing Yukawa operator of this kind once ω is expanded about its 4321-breaking vev.

The scalar potential of the model will lead the four $SU(2)_{L,1+2}$ Higgs doublets in \mathcal{H}_a^{22} (namely $\mathcal{H}_1^{22+}, \mathcal{H}_1^{22-}, \mathcal{H}_{15}^{22+}, \mathcal{H}_{15}^{22-}$) to have a small mixing with the corresponding $SU(2)_{L,3}$ Higgs doublets in H_1 , which are the fields driving the SM electroweak symmetry breaking (see section 4). As a consequence, the four neutral Higgs doublets in \mathcal{H}_a^{22} acquire a non-vanishing vev that, in general, we can write as

$$\langle \mathcal{H}_a^{22+} \rangle = \begin{pmatrix} 0 \\ \epsilon_h \eta_a^+ v \end{pmatrix}, \quad \langle \mathcal{H}_a^{22-} \rangle = \begin{pmatrix} \epsilon_h \eta_a^- v \\ 0 \end{pmatrix}, \quad (3.39)$$

where $v \approx 246$ GeV is the SM electroweak scale, $\epsilon_h \ll 1$ and $\eta_a^\pm = \mathcal{O}(1)$. The mass matrices of the SM fermions then arise from the combination of couplings of the third family to H_a , yielding 33 elements of $\mathcal{O}(v)$, and couplings of all other fermion bilinears to \mathcal{H}_a^{22} , yielding parametrically suppressed contributions of $\mathcal{O}(\epsilon_h v)$.

3.3 Fermion mass and mixing angle observables

Putting everything together from the previous subsections, one can derive the mass matrices of the SM fermions after electroweak symmetry breaking. For each of $f \in \{u, d, e\}$, the mass matrix assumes the following hierarchical structure

$$M_f \sim \frac{v}{\sqrt{2}} \begin{pmatrix} \epsilon_h \epsilon_L \epsilon_R & \epsilon_h \epsilon_L & \epsilon_h \epsilon_L \delta_f \\ \epsilon_h \epsilon_R & \epsilon_h & \epsilon_h \delta_f \\ 0 & 0 & 1 \end{pmatrix}, \quad (3.40)$$

where we have introduced the quantities

$$\delta_u = \frac{\lambda v_3}{m_{\xi_u^2}}, \quad \delta_d \ll \delta_u, \quad \delta_e = \frac{\lambda v_1}{m_{\xi_e^2}}, \quad (3.41)$$

where the hierarchy between δ_d and δ_u follows from the (natural) choice in eq. (3.32), that ω^{cb} gets the vev (a comparable $\delta_d \sim \delta_u$ would be achieved if a vev was also developed by the ω^{ts} component). Using matrix perturbation theory, one can extract the following overall scaling of the eigenvalues of such matrices, i.e. of the fermion masses in our model:

$$m_1 \sim \mathcal{O}(\epsilon_L \epsilon_R \epsilon_h), \quad (3.42)$$

$$m_2 \sim \mathcal{O}(\epsilon_h), \quad (3.43)$$

$$m_3 \sim \mathcal{O}(1). \quad (3.44)$$

The CKM angles scale as

$$V_{us} \sim \mathcal{O}(\epsilon_L), \quad (3.45)$$

$$V_{cb} \sim \mathcal{O}(\epsilon_h \delta_u), \quad (3.46)$$

$$V_{ub} \sim \mathcal{O}(\epsilon_L \epsilon_h \delta_u), \quad (3.47)$$

where we emphasize that each of these CKM elements admits a complex phase. The precise expressions are recorded in appendix A.

4 Anchoring the low scale

We now turn to the scalar sector of the model, in particular the mechanism by which a set of light electroweak doublets acquire their non-zero vevs (from which we identify the SM Higgs). By requiring limited tuning in this Higgs sector, we will place constraints on the various symmetry breaking scales of the model, thereby anchoring the masses of the lightest new physics particles close to the TeV scale.

4.1 The light-Higgs sector

The theory contains several scalar fields that, at the end of the breaking chain in figure 1, transform as doublets of $SU(2)_L$ and hence as SM Higgs fields. We denote as the “light-Higgs sector” the subset comprised of the four doublets $\{\mathcal{H}_a^{22\pm}\}$ (see section 3.2.2), i.e. those with second-family flavour indices, plus the four doublets from H_a . As anticipated, these two

sets mix because of the non-vanishing vev of the $\Sigma_{L,R}$ fields. More precisely, the doublets in $\mathcal{H}_a^{22\pm}$ mix with the doublets in H_1 but not H_{15} (at least not at the renormalisable level), and this mixing happens separately for the up-type and down-type components, i.e. only fields with the same $U(1)_R$ charges can mix.

In this light-Higgs sector we expect a single ‘ultra-light’ component to appear, that we identify with the effective SM-like Higgs. Without loss of generality, in order to simplify the notation, we assume that this ultra-light component can be identified with the up-type component of H_1 . In other words, we assume

$$|\langle H_1 \rangle| \gg |\langle H_{15} \rangle| \quad \text{and} \quad |\langle H_1^- \rangle| \gg |\langle H_1^+ \rangle|, \quad (4.1)$$

where $|\langle H_a \rangle|$ denotes the magnitude of the vev of the field H_a . To this end, we recall that it is sufficient that either H_1^- or H_1^+ acquire a non-vanishing vev in order to achieve the spontaneous symmetry breaking of electroweak symmetry and give non-vanishing masses to all the fermions. Indeed, via the \mathcal{R}_a and \mathcal{K}_a rotation matrices introduced above, the vev of a single (up or down) component of \mathcal{H}_a^{22} generates non-vanishing masses for both up and down quarks (and a similar mechanism holds for third-generation quarks). A non-vanishing vev for H_{15} is needed to generate the appropriate splitting between y_τ and y_b . However, the smallness of $y_{\tau,b}$ with respect to y_t ensures that this effect can easily be obtained with $|\langle H_{15} \rangle| \ll |\langle H_1 \rangle|$, hence with a tiny contribution of H_{15} to the electroweak vev (and, correspondingly, to the SM-like Higgs field).

As we shall see in the next section, the configuration in (4.1) can be obtained with a rather natural choice of parameters in the effective Higgs potential. The only critical point is to ensure $|\langle H_1 \rangle| \approx v$. This condition is what implies $\Lambda_\Sigma \lesssim 10$ TeV, anchoring the whole chain of symmetry breaking scales in figure 1.

4.1.1 Mixing and spectrum in the light-Higgs sector

The mixing between the $\{\mathcal{H}_a^{22\pm}\}$ fields and the components from H_1 is induced by the following interaction terms,

$$\mathcal{L} \supset \lambda_{H\Sigma}^1 \mathcal{H}_1^{22} \Sigma_L H_1 \Sigma_R + \lambda_{H\Sigma}^{15} \mathcal{H}_{15}^{22} \Sigma_L H_1 \Sigma_R + \text{h.c.}, \quad (4.2)$$

where we use the generic notation ‘ \mathcal{H}_a^{22} ’ to denote $SU(3)_{1+2}$ singlet scalar components originating from the UV Higgses \mathcal{H}_1 and \mathcal{H}_{15} . Recall that under the light-flavour deconstruction, $Sp(4)_L \rightarrow SU(2)_{L,1} \times SU(2)_{L,2}$, the Σ_L field decomposes as

$$\Sigma_L \sim \mathbf{4} \rightarrow (\mathbf{2}, \mathbf{1}) \oplus (\mathbf{1}, \mathbf{2}). \quad (4.3)$$

After $SU(2)_{L,1} \times SU(2)_{L,2} \rightarrow SU(2)_{L,1+2}$, this just gives two doublets of $SU(2)_{L,1+2}$ (see (3.25)). We assume that the vev of Σ_L occurs in the $(\mathbf{1}, \mathbf{2})$ component that couples to \mathcal{H}_a^{2j} , and likewise that the vev of Σ_R occurs in the $\mathbf{1}_{\pm 1/2}$ components of $SU(2)_{R,1} \times U(1)''_R$ that couple only to \mathcal{H}_a^{i2} . This way, once $\Sigma_{L,R}$ acquire their vevs, the mixing term in (4.2) selects only the \mathcal{H}_a^{22} components.

We now focus the attention on the up-type SU(4)-singlet Higgs fields, i.e. the fields that after $SU(2)_{L,1+2} \times SU(2)_{L,3} \rightarrow SU(2)_L$ behave as $SU(2)_L$ doublets with (SM) hypercharge $-1/2$. Their mass matrix, $\mathbf{M}_{\mathbf{u}}^2$, defined via

$$\mathcal{L} \supset (\vec{H}^-)^\dagger \mathbf{M}_{\mathbf{u}}^2 \vec{H}^- \tag{4.4}$$

where $\vec{H}^- = (\mathcal{H}_1^{22-}, \mathcal{H}_{15}^{22-}, H_1^-)$, assumes the form

$$\mathbf{M}_{\mathbf{u}}^2 = \begin{pmatrix} (M_1^u)^2 & 0 & \lambda_{H\Sigma}^1 |\langle \Sigma_L \rangle| |\langle \Sigma_R \rangle| \\ 0 & (M_{15}^u)^2 & \lambda_{H\Sigma}^{15} |\langle \Sigma_L \rangle| |\langle \Sigma_R \rangle| \\ \lambda_{H\Sigma}^1 |\langle \Sigma_L \rangle| |\langle \Sigma_R \rangle| & \lambda_{H\Sigma}^{15} |\langle \Sigma_L \rangle| |\langle \Sigma_R \rangle| & m_u^2 \end{pmatrix}. \tag{4.5}$$

A completely analogous structure holds for $\mathbf{M}_{\mathbf{d}}^2$, acting on the vector $(\mathcal{H}_1^{22+}, \mathcal{H}_{15}^{22+}, H_1^+)$, with identical off-diagonal entries and potentially different diagonal elements.¹³

The mass matrix $\mathbf{M}_{\mathbf{u}}^2$ can be diagonalized by an appropriate orthogonal rotation of the three fields,

$$O_u \mathbf{M}_{\mathbf{u}}^2 O_u^T = \text{diag}(M_{u_1}^2, M_{u_2}^2, -\mu_u^2). \tag{4.6}$$

Assuming $m_u^2, \lambda_{H\Sigma}^a |\langle \Sigma_{L,R} \rangle|^2 \ll (M_a^u)^2$, we find

$$\mu_u^2 \approx \sum_{a=1,15} (\theta_u^a)^2 (M_a^u)^2 - m_u^2, \tag{4.7}$$

where

$$\theta_u^a = \lambda_{H\Sigma}^a \frac{|\langle \Sigma_L \rangle| |\langle \Sigma_R \rangle|}{(M_a^u)^2}, \quad O_u \approx \begin{pmatrix} 1 & 0 & \theta_u^1 \\ 0 & 1 & \theta_u^{15} \\ -\theta_u^1 & -\theta_u^{15} & 1 \end{pmatrix}. \tag{4.8}$$

Electroweak symmetry breaking is achieved if either $\mathbf{M}_{\mathbf{u}}^2$ and/or $\mathbf{M}_{\mathbf{d}}^2$ develops small negative eigenvalues. This requires some tuning between the two terms in (4.7), or the analogous combination for $\mathbf{M}_{\mathbf{d}}^2$. It is natural to assume this happens only in one of the two mass matrices: we work under the hypothesis this happens only in $\mathbf{M}_{\mathbf{u}}^2$. In this limit, the effective mixing parameters defined in (3.39) assume the form

$$\epsilon_h = \sqrt{(\theta_u^1)^2 + (\theta_u^{15})^2}, \quad \eta_a^- \approx \frac{\theta_u^a}{\sqrt{(\theta_u^1)^2 + (\theta_u^{15})^2}} \frac{v_u}{v}, \quad \eta_a^+ = 0. \tag{4.9}$$

Here $v_u \propto \mu_u$ denotes the ‘fraction’ of the electroweak-breaking vev that is due to the H_1 field, while v denotes the total vev considering also the contribution from $\langle H_{15} \rangle$. The latter is controlled by independent parameters and can easily be tuned to be small, reaching the configuration (4.1).

¹³Generically, the components \mathcal{H}_1^{22-} and \mathcal{H}_{15}^{22-} are expected to mix and populate the 1-2 and 2-1 entries of the upper blocks of $\mathbf{M}_{\mathbf{u,d}}^2$. We work under the assumption that this mixing is absent as its only effect would be to re-define effective couplings $\lambda_{H\Sigma}^a$, leaving the following discussion essentially unchanged.

4.1.2 Constraints on the scales from the electroweak vacuum

The requirement that $\mu_u^2 \sim v^2$, with minimal tuning, allows us to derive a series of constraints on the symmetry breaking scales that appear in our setup. Assuming that both terms in (4.7) are of similar size implies

$$v^2 \sim \lambda_{H\Sigma}^2 \frac{\Lambda_\Sigma^4}{M_{\mathcal{H}}^2} \quad \rightarrow \quad \frac{\Lambda_\Sigma^2}{M_{\mathcal{H}}} \sim \frac{v}{\lambda_{H\Sigma}}, \quad (4.10)$$

where $\lambda_{H\Sigma}$ denotes generically $\lambda_{H\Sigma}^{1,15}$, and $M_{\mathcal{H}}$ generically denotes $M_{1,2}^u$. At the same time, the request $\epsilon_h \sim 10^{-2}$ from the Yukawa couplings implies

$$\epsilon_h \sim \lambda_{H\Sigma} \frac{\Lambda_\Sigma^2}{M_{\mathcal{H}}^2} \quad \rightarrow \quad \frac{M_{\mathcal{H}}}{\Lambda_\Sigma} \sim \left(\frac{\lambda_{H\Sigma}}{\epsilon_h} \right)^{1/2}. \quad (4.11)$$

The $\lambda_{H\Sigma}$ couplings cannot be arbitrarily small, since the operators in (4.2) are necessarily generated by quantum corrections: a natural lower bound is $|\lambda_{H\Sigma}| \gtrsim 10^{-2}$, which implies that Λ_Σ is at most as large as $M_{\mathcal{H}}$.

The last piece of information we need to take into account are the experimental bounds on the family non-universal electroweak gauge bosons (W', Z') generated by the breaking $SU(2)_{L,1+2} \times SU(2)_{L,3} \rightarrow SU(2)_L$. In particular from the stringent $Z' \rightarrow \ell\bar{\ell}$ bounds [31] we deduce $\Lambda_\Sigma \gtrsim 10$ TeV. All these constraint can be satisfied for $|\lambda_{H\Sigma}| \sim 0.01$ and

$$M_{\mathcal{H}} \sim \Lambda_\Sigma \sim 10 \text{ TeV}. \quad (4.12)$$

The range for $M_{\mathcal{H}}$ is well compatible with present bounds on heavy Higgs fields.

Combining these indications with the request $\epsilon_{L,R} \sim 10^{-1}$ from the light-fermion spectrum, and the bound $\Lambda_{12} \gtrsim 10^3$ TeV from flavour-changing processes involving the first two generations of quarks [32], we end up with a coherent spectrum where each of the four scales indicated in figure 1 are separated by one order of magnitude: starting from $\Lambda_{12} \sim 10^3$ TeV down to $\Lambda_{4321} \sim 1$ TeV, as summarised in figure 6. On general grounds, the scalar sector of this framework is stable under quantum corrections if the scalars at a given scale receive one-loop corrections only from scalars at the scale immediately above (and not from those at the higher scales) [6]. In our case, this condition is respected but for one exception, namely m_u^2 (i.e. the mass term of H_1), which could receive one-loop corrections from the $\Sigma_{L,R}$ fields. The natural expectation is thus $m_u \gtrsim 1$ TeV and not $m_u \lesssim v$. The model therefore requires some amount of fine-tuning in order to reproduce the observed value of the electroweak scale. However, this tuning is not worse than that present in any realistic SM extensions, given current bounds on direct searches for new physics. This is the manifestation of the so-called *little-hierarchy* problem [33] in our model.

4.2 Leptoquark phenomenology

We are now ready to analyse some of the phenomenological implications of our model at both low and high energies. As summarised in table 2, the model possesses a rich spectrum of new states at the TeV scale. A detailed analysis of the possible signatures of all these states in high-energy pp collisions is beyond the scope of this paper: these signatures vary

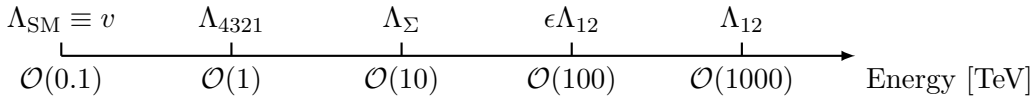


Figure 6. The relevant energy scales in our model, which are associated with different symmetry breaking steps (as detailed in figure 1), are each separated by roughly an order of magnitude.

a lot depending on the mass matrices of the new states which are poorly constrained by low-energy data. On the contrary, rather precise predictions can be obtained for processes mediated by the TeV-scale U_1 leptoquark (LQ) generated by the $4321 \rightarrow \text{SM}$ breaking. Analysing these predictions is also interesting in order to compare the expectations of our model with those of other 4321 completions.

In order to take advantage of a series of recent phenomenology analyses of 4321 models (see e.g. [30, 34, 35]), it is convenient to write the effective U_1 interactions with the SM fermions as

$$\mathcal{L}_{\text{eff}}^{\text{int}} = \frac{g_U}{\sqrt{2}} J_U^\mu U_\mu + \text{h.c.} \quad J_U^\mu = \left(\beta_L^{i\alpha} \bar{Q}_L^i \gamma^\mu L_L^\alpha + \beta_R \bar{b}_R \gamma^\mu \tau_R \right), \quad (4.13)$$

introducing the effective couplings g_U , $\beta_L^{i\alpha}$ and β_R . By convention, the quark doublet Q^i is written in the down-quark mass-eigenstate basis ($i = b, s, d$), the lepton doublet L_L^α is written in the charged-lepton mass-eigenstate basis ($\alpha = e, \mu, \tau$), and $\beta_L^{b\tau} \equiv 1$. Within our model, in the limit $\epsilon_h \rightarrow 0$, i.e. neglecting the mixing of the light families with the third, we have $g_U = g_4$, $|\beta_R| = 1$, and all the $\beta_L^{i\alpha}$ vanish but for $\beta_L^{b\tau}$.

As in all 4321 models, a key constraint on the flavour structure of the theory comes from the effective four-quark operators mediated by the TeV-scale color octet (coloron), which is also generated by the $4321 \rightarrow \text{SM}$ breaking. These effective operators are strongly constrained by $B_s - \bar{B}_s$ and $B_d - \bar{B}_d$ mixing (see e.g. [30, 35]). Satisfying these bounds requires the alignment of the third generation in the down sector, i.e. identifying the left-handed quark doublet charged under $\text{SU}(4)$ as

$$Q_L^3 \approx \begin{pmatrix} \sum_{q=u,c,t} V_{ub}^* q_L \\ b_L \end{pmatrix}. \quad (4.14)$$

This justifies, *a posteriori*, the choice of the down-mass eigenstate basis in eq. (4.13). Recall that, in our framework, this alignment condition follows from the hierarchy $\delta_d \ll \delta_u$, as in eq. (3.41) above, which is a natural consequence of assuming that the 4321 -breaking vev occurred in the component labelled ω^{cb} , as in eq. (3.32), given also that $|\langle \mathcal{H}_a^{22+} \rangle| = 0$. This implies that the heavy \rightarrow light mixing in the CKM matrix originates from the up-quark sector and that $\beta_L^{s\tau}, \beta_L^{d\tau}$ remain vanishing small, at the tree level, even if $\epsilon_h \neq 0$.

We emphasize that, in contrast to other 4321 models in the literature, the required down-alignment of the quark Yukawa matrices does not have to be imposed by hand in this model, but follows from a natural symmetry breaking structure that matches the deeper UV dynamics onto 4321 .

4.2.1 $R_{D^{(*)}}$ and $pp \rightarrow \tau^+ \tau^- + X$

Integrating out the LQ at tree-level leads to the following effective Lagrangian relevant to $b \rightarrow c \ell \nu$ decays:

$$\mathcal{L}_{b \rightarrow c} = -\frac{4G_F}{\sqrt{2}} V_{cb} \left[\left(1 + \mathcal{C}_{LL}^c\right) (\bar{c}_L \gamma_\mu b_L) (\bar{\tau}_L \gamma^\mu \nu_L) - 2 \mathcal{C}_{LR}^c (\bar{c}_L b_R) (\bar{\tau}_R \nu_L) \right], \quad (4.15)$$

where

$$\mathcal{C}_{LL}^c = \frac{v^2}{2\Lambda_U^2} \left(1 + \beta_L^{s\tau} \frac{V_{cs}}{V_{cb}}\right), \quad \mathcal{C}_{LR}^c = \beta_R^* \mathcal{C}_{LL}^c, \quad (4.16)$$

where we have written these Wilson coefficients in terms of the effective couplings introduced in eq. (4.13). The parameters $\mathcal{C}_{LL(R)}^c$ can be extracted from data via the lepton flavour universality (LFU) ratios $R_{D^{(*)}}$ using the following phenomenological expressions [35]:

$$\begin{aligned} \Delta R_D &\equiv \frac{R_D}{R_D^{\text{SM}}} - 1 = \text{Re} (2 \mathcal{C}_{LL}^c - 3.00 \mathcal{C}_{LR}^{c*}) + \mathcal{O}[(\mathcal{C}_{LL(R)}^c)^2], \\ \Delta R_{D^*} &\equiv \frac{R_{D^*}}{R_{D^*}^{\text{SM}}} - 1 = \text{Re} (2 \mathcal{C}_{LL}^c - 0.24 \mathcal{C}_{LR}^{c*}) + \mathcal{O}[(\mathcal{C}_{LL(R)}^c)^2]. \end{aligned} \quad (4.17)$$

According to the recent analysis of $b \rightarrow c \ell \nu$ data in [30], if $|\beta_R| = 1$ (as expected in our model) a very good fit to present data is obtained for $\beta_R = -1$, a phase choice that maximises the interference of left- and right-handed currents in eq. (4.17).¹⁴ The correspondingly preferred value of \mathcal{C}_{LL}^c is

$$\mathcal{C}_{LL}^c|_{\beta_R=-1}^{\text{exp}} = 0.03 \pm 0.01. \quad (4.18)$$

The maximal value of \mathcal{C}_{LL}^c in the model is determined by the experimental lower bound on M_U/g_U extracted from high-energy data. For large LQ masses, the high-energy process $pp \rightarrow \tau^+ \tau^- + X$, to which the LQ contributes via the t -channel exchange, turns out to be the most effective probe. From the recent CMS analysis in [36], focused on the LQ t -channel exchange amplitude, one extracts the bound $\Lambda_U \gtrsim 1.6$ TeV [30, 37], with a tantalizing 3σ excess for $\Lambda_U \approx 1.6$ TeV. Setting $\Lambda_U = 1.6$ TeV and $\beta_L^{s\tau} = 0$ we get $\mathcal{C}_{LL}^c|_{\beta_R=-1}^{\text{th}} = 0.012$ or, equivalently,

$$\Delta R_D \approx 6.0\%, \quad \Delta R_{D^*} \approx 2.7\%. \quad (4.19)$$

These values are already within the 2σ range determined by low-energy data, implying a significant agreement compared to the SM expectations in these observables. A further improvement could be obtained with a value of $\beta_L^{s\tau} \approx 0.01$, which could be generated beyond the tree level (see the next section).¹⁵ In this case $\mathcal{C}_{LL}^c|_{\beta_R=-1}^{\text{th}}$ could raise up to ≈ 0.015 , which is well within the 90%CL experimental range.

¹⁴The phase of β_R is a free parameter in our model determined by the relative sign of M_{33}^d and M_{33}^c .

¹⁵We emphasize that, in ‘bottom-up’ 4321 models designed to fit the central value of $R_{D^{(*)}}$, while being compatible with $pp \rightarrow \tau\tau$ data, the contribution to mixing from an additional vector-like fermion (not present in this model) is crucial [30]. See also footnote 9.

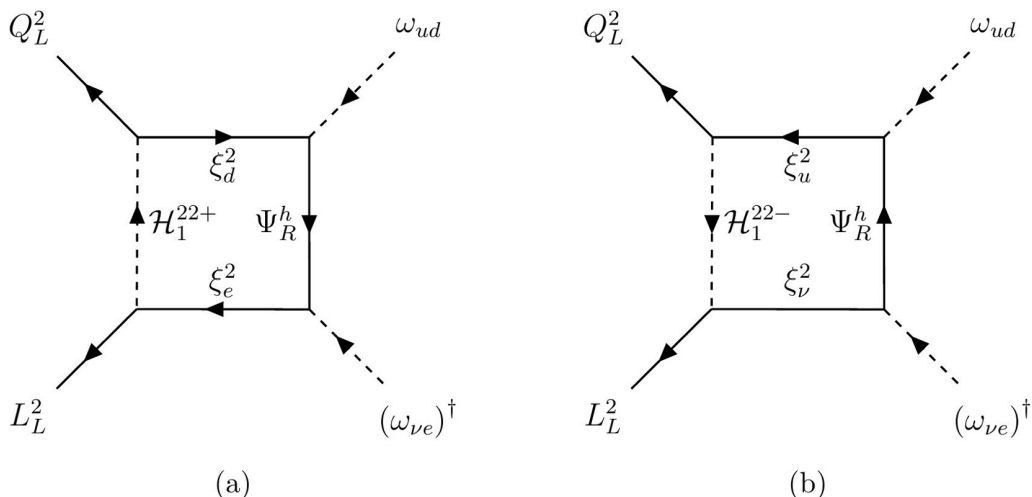


Figure 7. Box diagrams leading to an effective $\bar{Q}_L^2 \gamma^\mu L_L^2 U_\mu$ interaction, induced by the exchange of a (heavy) $SU(3)^I$ -singlet Higgs.

4.2.2 R_{K^*}

The LQ effective interaction in eq. (4.13) also leads to a tree-level contribution to $b \rightarrow s\mu^+\mu^-$ amplitudes that, in turn, induce non-vanishing corrections to the neutral-current LFU ratios R_K and R_{K^*} . However, as we shall see, these effects are naturally quite small in our setup.

Adopting the standard convention to define the $b \rightarrow s\mu^+\mu^-$ effective operators $O_{9,10}$ (see e.g. [9]), we get

$$\Delta C_9^{\mu\mu} = -\Delta C_{10}^{\mu\mu} = -\frac{v^2}{2\Lambda_U^2} \left(\frac{2\pi}{\alpha_{\text{em}}} \frac{\beta_L^{s\mu} \beta_L^{b\mu^*}}{V_{tb} V_{ts}^*} \right). \quad (4.20)$$

In terms of these modified Wilson coefficients, the LFU ratio R_K in the dilepton mass interval $m_{\ell\ell}^2 \in [1 \text{ GeV}^2, 6 \text{ GeV}^2]$ reads [35]:

$$\Delta R_K = R_K - 1 = 0.50 \text{ Re}(\Delta C_9^{\mu\mu})|_{\Lambda_U=1.6 \text{ TeV}} \approx 0.13 \times \text{Re} \left(\frac{\beta_L^{s\mu} \beta_L^{b\mu^*}}{10^{-3}} \right), \quad (4.21)$$

and in the same $m_{\ell\ell}^2$ interval we have $\Delta R_{K^*} \approx \Delta R_K$.

Within our model, a non-vanishing $\beta_L^{b\mu}$ is generated by the diagonalization of the lepton mass matrix,

$$|\beta_L^{b\mu}| \approx \left| \frac{\mathcal{M}_{23}^e}{\mathcal{M}_{33}^e} \right| = O(\epsilon_h \delta_e) < 10^{-1}. \quad (4.22)$$

On the contrary, the diagonalization of the quark mass matrices do not lead to a non-vanishing $\beta_L^{s\mu}$ in the limit of perfect down alignment.

An effective coupling of the LQ to second generation fermions is generated in the model beyond the tree level by the one-loop diagrams shown in figures 7 and 8. These one-loop diagrams generate a dimension-six operator of the type $\bar{Q}_L^i \gamma^\mu L_L^\alpha \omega_{ud}^{i3} D_\mu (\omega_{\nu e}^{3\alpha})^\dagger$ that, once

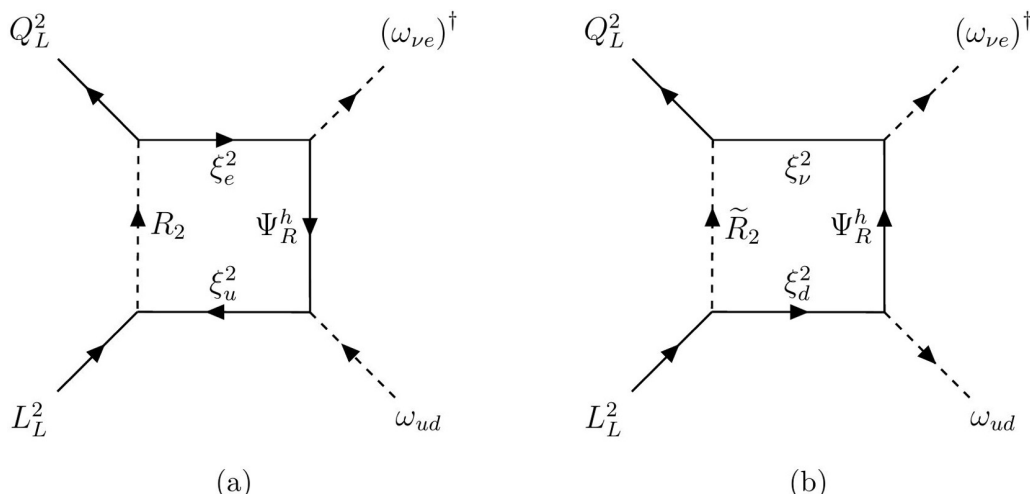


Figure 8. Box diagrams leading to an effective $\bar{Q}_L^2 \gamma^\mu L_L^2 U_\mu$ interaction, induced by the exchange of a (heavy) $SU(3)^l$ -triplet Higgs (these components originate from the decomposition of \mathcal{H}_{15}).

the ω fields acquire their vevs, leads to a non-vanishing $\bar{Q}_L^2 \gamma^\mu L_L^2 U_\mu$ effective interaction. The $\beta_L^{s\mu}$ thus generated can be written as

$$\beta_L^{s\mu} = \zeta \frac{\mathcal{M}_{22}^e \mathcal{M}_{22}^{d*}}{|\mathcal{M}_{22}^e| |\mathcal{M}_{22}^d|}, \quad (4.23)$$

where

$$\zeta \equiv \frac{\kappa_{1,15}^2 \lambda_q \lambda_\ell v_3 v_1}{16\sqrt{2}\pi^2} \sum_{\text{box diag.}} \Phi[M_{\mathcal{H}}, m_{\xi_\ell}, m_{\xi_q}], \quad (4.24)$$

with $\lambda_{q,\ell}$ denoting the couplings between ω , Ψ_R^h , and Ξ , and where the loop function is

$$\Phi[M_{\mathcal{H}}, m_{\xi_\ell}, m_{\xi_q}] \equiv - \frac{M_{\mathcal{H}}^2 - m_{\xi_\ell} m_{\xi_q} + m_{\xi_\ell} m_{\xi_q} \log\left(\frac{m_{\xi_\ell} m_{\xi_q}}{M_{\mathcal{H}}^2}\right)}{(m_{\xi_\ell} m_{\xi_q} - M_{\mathcal{H}}^2)^2}. \quad (4.25)$$

The sum over all relevant box diagrams yields

$$\begin{aligned} \zeta = \frac{\lambda_q \lambda_\ell v_3 v_1}{16\sqrt{2}\pi^2} & \left(\kappa_1^2 \Phi[M_{\mathcal{H}_1^{22+}}, m_{\xi_e}, m_{\xi_d}] + \kappa_{15}^2 \Phi[M_{\mathcal{H}_{15}^{22+}}, m_{\xi_e}, m_{\xi_d}] \right. \\ & + \kappa_1^2 \Phi[M_{\mathcal{H}_1^{22-}}, m_{\xi_\nu}, m_{\xi_u}] + \kappa_{15}^2 \Phi[M_{\mathcal{H}_{15}^{22-}}, m_{\xi_\nu}, m_{\xi_u}] \\ & + \kappa_{15}^2 \Phi[M_{R_2}, m_{\xi_e}, m_{\xi_u}] + \kappa_{15}^2 \Phi[M_{\tilde{R}_2}, m_{\xi_\nu}, m_{\xi_d}] \\ & \left. + \kappa_a \rightarrow \bar{\kappa}_a \right). \end{aligned} \quad (4.26)$$

The expression for $\beta_L^{s\mu}$ in (4.23) is suppressed both by the loop factor $1/(16\pi^2)$ and by the scale ratio $v_{1,3}^2/M_{\mathcal{H}}^2$. If all the heavy scalars running inside the loops have masses of $\mathcal{O}(10 \text{ TeV})$, as expected given that the corresponding scalar potential is characterised by the scale Λ_Σ , the corrections to $R_{K^{(*)}}$ should not exceed 1%. On general grounds, we thus

expect tiny modifications to $R_{K^{(*)}}$ below the detectable level, consistent with the recent findings of the LHCb Collaboration [19].

In specific regions of parameter space, mild cancellations in the effective potential could bring some of the scalar masses down to the TeV range, leading to larger corrections to $R_{K^{(*)}}$, close to the maximal values allowed by present data. For instance, a consistent benchmark point leading to $\Delta C_9^{\mu\mu} \sim -0.1$ (hence $\Delta R_K \approx -5\%$) is obtained for

$$\begin{aligned}
 m_{\xi_q^u} &\sim 1.4 \text{ TeV} , & m_{\xi_q^e} &\sim 1.1 \text{ TeV} , & v_3 &\sim 1.7 \text{ TeV} , & v_1 &\sim 1.7 \text{ TeV} , \\
 m_{\mathcal{H}_1^{22\pm}} &\sim 12.3 \text{ TeV} , & m_{\mathcal{H}_{15}^{22\pm}} &\sim 12.5 \text{ TeV} , & m_{R_2, \tilde{R}_2} &\sim 1.1 \text{ TeV} .
 \end{aligned}
 \tag{4.27}$$

We emphasize that, to achieve such a shift in $C_9^{\mu\mu}$, the masses of the R_2 and \tilde{R}_2 scalar leptoquarks are an order of magnitude lighter than their ‘natural’ size of $\mathcal{O}(10 \text{ TeV})$.

5 Conclusion and outlook

In this paper we explore a new kind of gauge model for explaining the origin of flavour in the Standard Model (SM). We suppose that physics in the UV is described by gauge interactions that unify quarks and leptons but in a fundamentally flavour non-universal way. We invoke a “2+1” family structure i.e. with the third family coupling to its own set of UV gauge bosons. On the other hand, within the first two generations we employ the rigid structure of electroweak-flavour unification. This unifying symmetry naturally controls flavour-changing processes in the 1–2 sector to be small, while generating hierarchical masses and mixing angles in the 1–2 sector through symmetry breaking steps at high energy scales. At lower energies of $\mathcal{O}(10 \text{ TeV})$, the light- and heavy-sectors are linked together, to match onto a non-universal ‘4321 model’, which is finally broken to the SM near the TeV scale.

A model of this kind, while seemingly quite complex, is well motivated on general grounds by our current knowledge of particle physics in both the electroweak and flavour sectors. In summary, it naturally explains:

- the spectrum of quarks and leptons and their seemingly *ad hoc* pattern of hypercharges, within each SM family, via enlarged SU(4) colour symmetries;
- the observed hierarchical pattern of fermion masses and quark mixing angles, with $\mathcal{O}(1)$ Yukawa couplings for the third family;
- why there exist two generations that are ‘light’ i.e. with suppressed Yukawa couplings $\ll 1$, that are in this sense similar from the point of view of the Higgs sector;
- why flavour-changing transitions in this 1–2 sector are consistent with the SM, probing new physics contributions up to very high (effective) scales;
- why a SM Higgs boson of $\mathcal{O}(0.1 \text{ TeV})$ mass is not unnatural (beyond an unavoidable tuning of about 1 part in 100 as per the ‘little hierarchy problem’), given our ladder of symmetry breaking scales can be anchored at the TeV scale.

The output of such a model-building framework, from the phenomenological perspective, is a new physics sector coupled dominantly to the third generation fermions, in the vicinity of the TeV scale.

We have not comprehensively studied the phenomenology of the new physics particles in this work, but rather pointed out the most obvious effects. One of the lightest new particles is a U_1 vector leptoquark with flavour non-universal couplings. As in other 4321 models, the leptoquark parameter space is cornered by high- p_T data and complementary constraints on the coloron and Z' gauge bosons that necessarily accompany it. An interesting aspect of this model, compared to generic 4321 constructions, is the possibility to justify the down-alignment of the heavy $SU(4)$ gauge bosons –phenomenologically required to satisfy the tight $\Delta F = 2$ bounds — as a result of the vacuum structure of the link fields mediating $4321 \rightarrow \text{SM}$ breaking. These link fields carry remnant light-flavour indices as a result of the high-scale electroweak-flavour unification.

We discussed the extent to which the U_1 leptoquark can explain the hints of new physics in charged-current ($b \rightarrow c\tau\nu$) B -meson decays. The model can naturally accommodate a 6% and 3% increase in R_D and $R_{D^{(*)}}$ respectively. While not matching the current central values of these observables, these effects significantly ease the tension with respect to the SM predictions. The relative impact on $b \rightarrow s\mu\mu$ amplitudes is naturally smaller, except for very specific regions of the parameter range where it can reach at most the few % level, consistent with recent findings [19].

Beyond these particles, there are other states near the TeV scale that differ from other 4321 models, most notably in the scalar sector. For example, we have a suite of heavy scalar particles in the same representation as the SM Higgs, but with heavier masses and with $\mathcal{O}(1)$ Yukawa couplings to the second generation fermions. There is also a set of vector-like fermions, needed to generate the CKM rotation angles involving the third family, which are also expected to be rather light (certainly if the U_1 leptoquark is to mediate any appreciable contribution to $b \rightarrow s\mu\mu$ transitions). We save phenomenological explorations of the high- p_T signatures of these particles for future work.

Another direction for future work, in a more theoretical vein, is to explore the perturbativity of this model (and other UV complete models of its ilk) up to scales of order 1000 TeV (at least), where the 1–2 flavour sector is expected to originate dynamically (recall figure 6). This requires a complete RG-evolution of the gauge and Yukawa couplings in the model, and a systematic study of the model parameter space.

Finally, we reiterate that, even though 4321-like models grew out of the observed anomalies in B -meson decays, the symmetry breaking patterns and UV dynamics that we study here remain well-motivated even in the absence of any of the anomalies. The hypothesis of flavour non-universal gauge interactions near the TeV scale is an attractive starting point for explaining the flavour puzzle, which is simultaneously consistent with the absence of new physics signals in high energy searches at the LHC, and the experimental constraints from precision flavour physics. Moreover, if one tries to reconcile this hypothesis of gauge non-universality with a quasi-natural fundamental Higgs up to scales of $\mathcal{O}(1 - 10)$ TeV, as we do here, then it can be argued that *all* natural options feature $SU(4)$ unification in the third family, and consequently U_1 leptoquarks, below ~ 10 TeV [38].

Acknowledgments

JD is grateful to J. Tooby-Smith for discussions and for collaboration on related work. This work is funded by the European Research Council (ERC) under the European Union’s Horizon 2020 research and innovation programme under grant agreement 833280 (FLAY), and by the Swiss National Science Foundation (SNF) under contract 200020-204428.

A Formulae for fermion masses and mixing angles

In this appendix we record the precise formulae for the quark and charged lepton masses and mixings in our model, in terms of the fundamental UV couplings of the theory, obtained by tree-level EFT matching at each symmetry breaking step.

We begin by writing the mass matrices M^f for each type of fermion, $f \in \{u, d, e\}$. There are contributions from both the ‘light-Higgs sector’ fields $\{\mathcal{H}_a^{22\pm}\}$, which recall get vevs $|\langle \mathcal{H}_a^{22\pm} \rangle| = \epsilon_h \eta_a^\pm v$, and from $\{H_a\}$, for which we parametrize the vevs as

$$\langle H_1 \rangle = v_1^- B_1 \otimes C_2 - v_1^+ B_2 \otimes C_1, \quad (\text{A.1})$$

$$\langle H_{15} \rangle = \left(\sum_{i=1}^3 A_i \otimes A_i^* - 3A_4 \otimes A_4^* \right) \otimes \left(v_{15}^- B_1 \otimes C_2 - v_{15}^+ B_2 \otimes C_1 \right), \quad (\text{A.2})$$

using the bases defined in section 2.1 of the main text. While in the main text we adopt the hypothesis that $\eta_a^+ = 0$, as given by eq. (4.9), in this appendix we give general formulae valid for any η_a^\pm .

Each mass matrix can be decomposed into the following ‘2+1’ block structure

$$\sqrt{2}M^f = \begin{pmatrix} \epsilon_h \widehat{\mathcal{M}}^f & \epsilon_h \delta_f \widehat{\mathbf{n}}^f \\ \mathbf{0}^T & M_{33}^f \end{pmatrix}, \quad (\text{A.3})$$

where recall the δ_f parameters are defined in eq. (3.41). Defining $\Gamma_1 = 1$ and $\Gamma_{15} = -3$, which encodes the relative values of the Higgs vevs on the charged leptons, and summing over $a \in \{1, 15\}$, we have

$$M_{33}^u = y_a^3 v_a^- + \bar{y}_a^3 v_a^{+*}, \quad (\text{A.4})$$

$$M_{33}^d = y_a^3 v_a^+ + \bar{y}_a^3 v_a^{-*}, \quad (\text{A.5})$$

$$M_{33}^e = \Gamma_a [y_a^3 v_a^+ + \bar{y}_a^3 v_a^{-*}]. \quad (\text{A.6})$$

The U(2)-breaking vectors $\widehat{\mathbf{n}}^f$ that mix the light families with the third are each given by

$$\widehat{\mathbf{n}}^f = \begin{pmatrix} \epsilon_L & 0 \\ 0 & 1 \end{pmatrix} \mathbf{n}^f, \quad (\text{A.7})$$

where

$$\mathbf{n}^u = v \left(\beta_L^a (\kappa_a \eta_a^- + \bar{\kappa}_a \eta_a^{+*}), \quad (\kappa_a \eta_a^- + \bar{\kappa}_a \eta_a^{+*}) \right)^T = (n_1^u, n_2^u)^T, \quad (\text{A.8})$$

$$\mathbf{n}^d = v \left(\beta_L^a (\kappa_a \eta_a^+ + \bar{\kappa}_a \eta_a^{-*}), \quad (\kappa_a \eta_a^+ + \bar{\kappa}_a \eta_a^{-*}) \right)^T = (n_1^d, n_2^d)^T, \quad (\text{A.9})$$

$$\mathbf{n}^e = v \left(\beta_L^a \Gamma_a (\kappa_a \eta_a^+ + \bar{\kappa}_a \eta_a^{-*}), \quad \Gamma_a (\kappa_a \eta_a^+ + \bar{\kappa}_a \eta_a^{-*}) \right)^T = (n_1^e, n_2^e)^T, \quad (\text{A.10})$$

still summing over $a \in \{1, 15\}$ in each term (the relative weighting by $\beta_L^{1,15}$ means that the first component of these vectors is not simply a rescaling of the second component by the same factor).

Finally, we define the upper-left 2-by-2 blocks, whose structures are generated by the EWFU mechanism. It is convenient to pull out the overall $\epsilon_{L,R}$ dependence, by defining

$$\widehat{\mathcal{M}}^f = \begin{pmatrix} \epsilon_L \epsilon_R \mathcal{M}_{11}^f & \epsilon_L \mathcal{M}_{12}^f \\ \epsilon_R \mathcal{M}_{21}^f & \mathcal{M}_{22}^f \end{pmatrix}. \quad (\text{A.11})$$

Then the ‘reduced’ matrix elements are

$$\mathcal{M}_{11}^u = v [(\beta_{LR}^a + 2\beta_L^a \beta_R^a) z_+ + (\beta_{LR}^{a*} + 2\beta_L^a \beta_R^{a*}) z_-] (y_a^l \eta_a^- + \bar{y}_a^l \eta_a^{+*}), \quad (\text{A.12})$$

$$\mathcal{M}_{12}^u = v \beta_L^a (y_a^l \eta_a^- + \bar{y}_a^l \eta_a^{+*}), \quad (\text{A.13})$$

$$\mathcal{M}_{21}^u = v (z_+ \beta_R^a + z_- \beta_R^{a*}) (y_a^l \eta_a^- + \bar{y}_a^l \eta_a^{+*}), \quad (\text{A.14})$$

$$\mathcal{M}_{22}^u = v (y_a^l \eta_a^- + \bar{y}_a^l \eta_a^{+*}). \quad (\text{A.15})$$

To obtain the corresponding formulae for \mathcal{M}^d , simply replace $y_a^l \eta_a^- + \bar{y}_a^l \eta_a^{+*}$ by $y_a^l \eta_a^+ + \bar{y}_a^l \eta_a^{-*}$ everywhere. To obtain the formulae for \mathcal{M}^e , additionally insert factors of Γ_a .

Using matrix perturbation theory, we calculate the eigenvalues of these matrices, to give the mass formulae:

$$m_t = |M_{33}^u|, \quad (\text{A.16})$$

$$m_b = |M_{33}^d|, \quad (\text{A.17})$$

$$m_\tau = |M_{33}^e|, \quad (\text{A.18})$$

$$m_c = \epsilon_h |\mathcal{M}_{22}^u|, \quad (\text{A.19})$$

$$m_s = \epsilon_h |\mathcal{M}_{22}^d|, \quad (\text{A.20})$$

$$m_\mu = \epsilon_h |\mathcal{M}_{22}^e|, \quad (\text{A.21})$$

$$m_u = \epsilon_h \epsilon_L \epsilon_R \frac{|\det(\mathcal{M}^u)|}{|\mathcal{M}_{22}^u|}, \quad (\text{A.22})$$

$$m_d = \epsilon_h \epsilon_L \epsilon_R \frac{|\det(\mathcal{M}^d)|}{|\mathcal{M}_{22}^d|}, \quad (\text{A.23})$$

$$m_e = \epsilon_h \epsilon_L \epsilon_R \frac{|\det(\mathcal{M}^e)|}{|\mathcal{M}_{22}^e|}. \quad (\text{A.24})$$

As described in the main text, the rough hierarchies are, in terms of our small model parameters $\epsilon_{L,R,h}$, given by $m_2/m_3 \sim \epsilon_h$ and $m_1/m_2 \sim \epsilon_L \epsilon_R$.

The CKM matrix is a little more involved. We have, firstly, the unsuppressed CKM elements on the leading diagonal:

$$V_{ud} = \frac{\mathcal{M}_{22}^{d*} \mathcal{M}_{22}^u \det(\mathcal{M}^d \mathcal{M}^{u*})}{|\mathcal{M}_{22}^d \mathcal{M}_{22}^u \det(\mathcal{M}^d \mathcal{M}^u)|}, \quad (\text{A.25})$$

$$V_{cs} = \frac{\mathcal{M}_{22}^d \mathcal{M}_{22}^{u*}}{|\mathcal{M}_{22}^d \mathcal{M}_{22}^u|}, \quad (\text{A.26})$$

$$V_{tb} = \frac{M_{33}^u M_{33}^{d*}}{|M_{33}^u M_{33}^d|}. \quad (\text{A.27})$$

The next largest elements are the Cabibbo-suppressed CKM elements mixing the first and second generations, where we emphasise the suppression by $\epsilon_L \sim \lambda$ in blue,

$$V_{us} = \frac{1}{|\mathcal{M}_{22}^d \mathcal{M}_{22}^u|} \left(\mathcal{M}_{12}^d \mathcal{M}_{22}^u \frac{\det(\mathcal{M}^{u*})}{|\det(\mathcal{M}^u)|} - \mathcal{M}_{22}^d \mathcal{M}_{12}^u \right) \epsilon_L, \quad (\text{A.28})$$

$$V_{cd} = \frac{1}{|\mathcal{M}_{22}^d \mathcal{M}_{22}^u|} \left(\mathcal{M}_{12}^{u*} \mathcal{M}_{22}^{d*} \frac{\det(\mathcal{M}^d)}{|\det(\mathcal{M}^d)|} - \mathcal{M}_{22}^{u*} \mathcal{M}_{12}^{d*} \right) \epsilon_L. \quad (\text{A.29})$$

Next, the CKM elements mixing the second and third generation are

$$V_{cb} = \frac{1}{|M_{33}^d \mathcal{M}_{22}^u M_{33}^u|} \left(n_2^d \mathcal{M}_{22}^{u*} |M_{33}^u| \delta_d - M_{33}^d n_2^u |\mathcal{M}_{22}^u| \delta_u \right), \quad (\text{A.30})$$

$$V_{ts} = \frac{1}{|M_{33}^d \mathcal{M}_{22}^d M_{33}^u|} \left(n_2^{u*} \mathcal{M}_{22}^d |M_{33}^d| \delta_u - M_{33}^{u*} n_2^{d*} |\mathcal{M}_{22}^d| \delta_d \right), \quad (\text{A.31})$$

where the suppression by factors of $\delta_{u,d} \sim \lambda^2$ are denoted in red. Finally, we have the CKM elements mixing the first and third family,

$$V_{ub} = \frac{1}{|M_{33}^d|} \left(\frac{n_1^d \mathcal{M}_{22}^u \det(\mathcal{M}^{u*})}{|\mathcal{M}_{22}^u| |\det(\mathcal{M}^u)|} \delta_d - \frac{n_2^d \mathcal{M}_{12}^u}{|\mathcal{M}_{22}^u|} \delta_d - \frac{M_{33}^d n_1^u}{|M_{33}^u|} \delta_u \right) \epsilon_L, \quad (\text{A.32})$$

$$V_{td} = \frac{1}{|M_{33}^u|} \left(\frac{n_1^{u*} \mathcal{M}_{22}^{d*} \det(\mathcal{M}^d)}{|\mathcal{M}_{22}^d| |\det(\mathcal{M}^d)|} \delta_u - \frac{n_2^{u*} \mathcal{M}_{12}^{d*}}{|\mathcal{M}_{22}^d|} \delta_u - \frac{M_{33}^{u*} n_1^{d*}}{|M_{33}^d|} \delta_d \right) \epsilon_L, \quad (\text{A.33})$$

which, as expected, are doubly-suppressed.

For completeness, we conclude this appendix by giving a formula for the Jarlskog invariant $J = \text{Im}[V_{us} V_{cb} V_{ub}^* V_{cs}^*]$, which captures the CP -violating phase in the CKM matrix. First defining

$$\mathcal{J}_1 \equiv \left(\mathcal{M}_{22}^d \mathcal{M}_{12}^u |\det(\mathcal{M}^u)| - \mathcal{M}_{12}^d \mathcal{M}_{22}^u \det(\mathcal{M}^{u*}) \right), \quad (\text{A.34})$$

$$\mathcal{J}_2 \equiv \left[|M_{33}^u| n_1^{d*} \mathcal{M}_{22}^{u*} \det(\mathcal{M}^u) - |\det(\mathcal{M}^u)| \left(|M_{33}^u| \mathcal{M}_{12}^u n_2^d + |\mathcal{M}_{22}^u| |M_{33}^d| n_1^u \frac{\delta_u}{\delta_d} \right)^* \right], \quad (\text{A.35})$$

which are generically $\mathcal{O}(1)$ quantities, we have

$$J = \left[\frac{M_{33}^d \mathcal{M}_{22}^u \mathcal{M}_{22}^{d*} n_2^u}{|\mathcal{M}_{22}^u|^3 |\det(\mathcal{M}^u)| \mathcal{M}_{22}^d M_{33}^d M_{33}^u|^2} - \frac{|M_{33}^u| \mathcal{M}_{22}^{d*} n_2^d}{|\mathcal{M}_{22}^u|^2 |\det(\mathcal{M}^u)| \mathcal{M}_{22}^d M_{33}^d M_{33}^u|^2} \frac{\delta_d}{\delta_u} \right] \mathcal{J}_1 \mathcal{J}_2 \delta_u \delta_d \epsilon_L^2 \quad (\text{A.36})$$

B Basis of $\text{Sp}(4)$ generators

For ease of reference, a basis for the 10-dimensional Lie algebra $\mathfrak{sp}(4)$, in the defining representation, is

$$\lambda_1 = \frac{1}{2} \begin{pmatrix} 1 & 0 & 0 & 0 \\ 0 & 0 & 0 & 0 \\ 0 & 0 & -1 & 0 \\ 0 & 0 & 0 & 0 \end{pmatrix}, \quad \lambda_2 = \frac{1}{2} \begin{pmatrix} 0 & 0 & 0 & 0 \\ 0 & 1 & 0 & 0 \\ 0 & 0 & 0 & 0 \\ 0 & 0 & 0 & -1 \end{pmatrix}, \quad (\text{B.1})$$

$$\lambda_3 = \frac{1}{2\sqrt{2}} \begin{pmatrix} 0 & 1 & 0 & 0 \\ 1 & 0 & 0 & 0 \\ 0 & 0 & 0 & -1 \\ 0 & 0 & -1 & 0 \end{pmatrix}, \quad \lambda_4 = \frac{1}{2\sqrt{2}} \begin{pmatrix} 0 & i & 0 & 0 \\ -i & 0 & 0 & 0 \\ 0 & 0 & 0 & i \\ 0 & 0 & -i & 0 \end{pmatrix}, \quad (\text{B.2})$$

$$\lambda_5 = \frac{1}{2} \begin{pmatrix} 0 & 0 & 1 & 0 \\ 0 & 0 & 0 & 0 \\ 1 & 0 & 0 & 0 \\ 0 & 0 & 0 & 0 \end{pmatrix}, \quad \lambda_6 = \frac{1}{2} \begin{pmatrix} 0 & 0 & i & 0 \\ 0 & 0 & 0 & 0 \\ -i & 0 & 0 & 0 \\ 0 & 0 & 0 & 0 \end{pmatrix}, \quad (\text{B.3})$$

$$\lambda_7 = \frac{1}{2} \begin{pmatrix} 0 & 0 & 0 & 0 \\ 0 & 0 & 0 & 1 \\ 0 & 0 & 0 & 0 \\ 0 & 1 & 0 & 0 \end{pmatrix}, \quad \lambda_8 = \frac{1}{2} \begin{pmatrix} 0 & 0 & 0 & 0 \\ 0 & 0 & 0 & i \\ 0 & 0 & 0 & 0 \\ 0 & -i & 0 & 0 \end{pmatrix}, \quad (\text{B.4})$$

$$\lambda_9 = \frac{1}{2\sqrt{2}} \begin{pmatrix} 0 & 0 & 0 & 1 \\ 0 & 0 & 1 & 0 \\ 0 & 1 & 0 & 0 \\ 1 & 0 & 0 & 0 \end{pmatrix}, \quad \lambda_{10} = \frac{1}{2\sqrt{2}} \begin{pmatrix} 0 & 0 & 0 & i \\ 0 & 0 & i & 0 \\ 0 & -i & 0 & 0 \\ -i & 0 & 0 & 0 \end{pmatrix} \quad (\text{B.5})$$

The normalization is such that

$$\text{Tr}(\lambda_a \lambda_b) = \frac{1}{2} \delta_{ab}. \quad (\text{B.6})$$

Open Access. This article is distributed under the terms of the Creative Commons Attribution License ([CC-BY 4.0](https://creativecommons.org/licenses/by/4.0/)), which permits any use, distribution and reproduction in any medium, provided the original author(s) and source are credited. SCOAP³ supports the goals of the International Year of Basic Sciences for Sustainable Development.

References

- [1] H. Georgi and S.L. Glashow, *Unity of All Elementary Particle Forces*, *Phys. Rev. Lett.* **32** (1974) 438 [[INSPIRE](#)].
- [2] C.D. Froggatt and H.B. Nielsen, *Hierarchy of Quark Masses, Cabibbo Angles and CP Violation*, *Nucl. Phys. B* **147** (1979) 277 [[INSPIRE](#)].
- [3] G.R. Dvali and M.A. Shifman, *Families as neighbors in extra dimension*, *Phys. Lett. B* **475** (2000) 295 [[hep-ph/0001072](#)] [[INSPIRE](#)].
- [4] G. Panico and A. Pomarol, *Flavor hierarchies from dynamical scales*, *JHEP* **07** (2016) 097 [[arXiv:1603.06609](#)] [[INSPIRE](#)].
- [5] M. Bordone, C. Cornella, J. Fuentes-Martín and G. Isidori, *A three-site gauge model for flavor hierarchies and flavor anomalies*, *Phys. Lett. B* **779** (2018) 317 [[arXiv:1712.01368](#)] [[INSPIRE](#)].
- [6] L. Allwicher, G. Isidori and A.E. Thomsen, *Stability of the Higgs Sector in a Flavor-Inspired Multi-Scale Model*, *JHEP* **01** (2021) 191 [[arXiv:2011.01946](#)] [[INSPIRE](#)].
- [7] R. Barbieri, *A View of Flavour Physics in 2021*, *Acta Phys. Polon. B* **52** (2021) 789 [[arXiv:2103.15635](#)] [[INSPIRE](#)].

- [8] J. Fuentes-Martín et al., *Flavor hierarchies, flavor anomalies, and Higgs mass from a warped extra dimension*, *Phys. Lett. B* **834** (2022) 137382 [[arXiv:2203.01952](#)] [[INSPIRE](#)].
- [9] D. London and J. Matias, *B Flavour Anomalies: 2021 Theoretical Status Report*, *Ann. Rev. Nucl. Part. Sci.* **72** (2022) 37 [[arXiv:2110.13270](#)] [[INSPIRE](#)].
- [10] D. Buttazzo, A. Greljo, G. Isidori and D. Marzocca, *B-physics anomalies: a guide to combined explanations*, *JHEP* **11** (2017) 044 [[arXiv:1706.07808](#)] [[INSPIRE](#)].
- [11] L. Di Luzio, A. Greljo and M. Nardecchia, *Gauge leptoquark as the origin of B-physics anomalies*, *Phys. Rev. D* **96** (2017) 115011 [[arXiv:1708.08450](#)] [[INSPIRE](#)].
- [12] A. Greljo and B.A. Stefanek, *Third family quark-lepton unification at the TeV scale*, *Phys. Lett. B* **782** (2018) 131 [[arXiv:1802.04274](#)] [[INSPIRE](#)].
- [13] J.C. Pati and A. Salam, *Lepton Number as the Fourth Color*, *Phys. Rev. D* **10** (1974) 275 [[INSPIRE](#)].
- [14] R. Barbieri et al., *U(2) and Minimal Flavour Violation in Supersymmetry*, *Eur. Phys. J. C* **71** (2011) 1725 [[arXiv:1105.2296](#)] [[INSPIRE](#)].
- [15] G. Isidori and D.M. Straub, *Minimal Flavour Violation and Beyond*, *Eur. Phys. J. C* **72** (2012) 2103 [[arXiv:1202.0464](#)] [[INSPIRE](#)].
- [16] J. Fuentes-Martín and P. Stangl, *Third-family quark-lepton unification with a fundamental composite Higgs*, *Phys. Lett. B* **811** (2020) 135953 [[arXiv:2004.11376](#)] [[INSPIRE](#)].
- [17] M. Fernández Navarro and S.F. King, *B-anomalies in a twin Pati-Salam theory of flavour including the 2022 LHCb $R_{K^{(*)}}$ analysis*, *JHEP* **02** (2023) 188 [[arXiv:2209.00276](#)] [[INSPIRE](#)].
- [18] J. Davighi and J. Tooby-Smith, *Electroweak flavour unification*, *JHEP* **09** (2022) 193 [[arXiv:2201.07245](#)] [[INSPIRE](#)].
- [19] LHCb collaboration, *Measurement of lepton universality parameters in $B^+ \rightarrow K^+ \ell^+ \ell^-$ and $B^0 \rightarrow K^{*0} \ell^+ \ell^-$ decays*, [arXiv:2212.09153](#) [[INSPIRE](#)].
- [20] B.C. Allanach, B. Gripaios and J. Tooby-Smith, *Semisimple extensions of the Standard Model gauge algebra*, *Phys. Rev. D* **104** (2021) 035035 [*Erratum ibid.* **106** (2022) 019901] [[arXiv:2104.14555](#)] [[INSPIRE](#)].
- [21] E. Witten, *An SU(2) Anomaly*, *Phys. Lett. B* **117** (1982) 324 [[INSPIRE](#)].
- [22] I. García-Etxebarria and M. Montero, *Dai-Freed anomalies in particle physics*, *JHEP* **08** (2019) 003 [[arXiv:1808.00009](#)] [[INSPIRE](#)].
- [23] J. Davighi, B. Gripaios and N. Lohitsiri, *Global anomalies in the Standard Model(s) and Beyond*, *JHEP* **07** (2020) 232 [[arXiv:1910.11277](#)] [[INSPIRE](#)].
- [24] J. Davighi, *Gauge flavour unification: from the flavour puzzle to stable protons*, in the proceedings of the *35th Recontres de Physique de la Vallée d'Aoste*, La Thuile Italy, March 6–12 (2022) [[arXiv:2206.04482](#)] [[INSPIRE](#)].
- [25] C.T. Hill, P.A.N. Machado, A.E. Thomsen and J. Turner, *Scalar Democracy*, *Phys. Rev. D* **100** (2019) 015015 [[arXiv:1902.07214](#)] [[INSPIRE](#)].
- [26] C.T. Hill, P.A.N. Machado, A.E. Thomsen and J. Turner, *Where are the Next Higgs Bosons?*, *Phys. Rev. D* **100** (2019) 015051 [[arXiv:1904.04257](#)] [[INSPIRE](#)].
- [27] L. Di Luzio et al., *Maximal Flavour Violation: a Cabibbo mechanism for leptoquarks*, *JHEP* **11** (2018) 081 [[arXiv:1808.00942](#)] [[INSPIRE](#)].

- [28] M. Bordone, C. Cornella, J. Fuentes-Martín and G. Isidori, *Low-energy signatures of the PS^3 model: from B -physics anomalies to LFV*, *JHEP* **10** (2018) 148 [[arXiv:1805.09328](#)] [[INSPIRE](#)].
- [29] J. Fuentes-Martín, G. Isidori, J. Pagès and B.A. Stefanek, *Flavor non-universal Pati-Salam unification and neutrino masses*, *Phys. Lett. B* **820** (2021) 136484 [[arXiv:2012.10492](#)] [[INSPIRE](#)].
- [30] J. Aebischer et al., *Confronting the vector leptoquark hypothesis with new low- and high-energy data*, *Eur. Phys. J. C* **83** (2023) 153 [[arXiv:2210.13422](#)] [[INSPIRE](#)].
- [31] CMS collaboration, *Search for resonant and nonresonant new phenomena in high-mass dilepton final states at $\sqrt{s} = 13$ TeV*, *JHEP* **07** (2021) 208 [[arXiv:2103.02708](#)] [[INSPIRE](#)].
- [32] G. Isidori, Y. Nir and G. Perez, *Flavor Physics Constraints for Physics Beyond the Standard Model*, *Ann. Rev. Nucl. Part. Sci.* **60** (2010) 355 [[arXiv:1002.0900](#)] [[INSPIRE](#)].
- [33] G.F. Giudice, *The Dawn of the Post-Naturalness Era*, in *From My Vast Repertoire ...: Guido Altarelli's Legacy*, A. Levy et al. eds., World Scientific (2019), pp. 267–292 [[DOI:10.1142/9789813238053_0013](#)] [[arXiv:1710.07663](#)] [[INSPIRE](#)].
- [34] C. Cornella, J. Fuentes-Martín and G. Isidori, *Revisiting the vector leptoquark explanation of the B -physics anomalies*, *JHEP* **07** (2019) 168 [[arXiv:1903.11517](#)] [[INSPIRE](#)].
- [35] C. Cornella et al., *Reading the footprints of the B -meson flavor anomalies*, *JHEP* **08** (2021) 050 [[arXiv:2103.16558](#)] [[INSPIRE](#)].
- [36] CMS collaboration, *The search for a third-generation leptoquark coupling to a τ lepton and a b quark through single, pair and nonresonant production at $\sqrt{s} = 13$ TeV*, *CMS-PAS-EXO-19-016* (2022) [[INSPIRE](#)].
- [37] U. Haisch, L. Schnell and S. Schulte, *Drell-Yan production in third-generation gauge vector leptoquark models at NLO+PS in QCD*, *JHEP* **02** (2023) 070 [[arXiv:2209.12780](#)] [[INSPIRE](#)].
- [38] J. Davighi and G. Isidori, *Non-universal gauge interactions addressing the inescapable link between Higgs and Flavour*, [arXiv:2303.01520](#) [[INSPIRE](#)].